5

Recent Developments in Spectroscopic and Chemical Characterization of Cellulose

Rajai H. Atalla
USDA Forest Service and University of Wisconsin, Madison. Wisconsin, U.S.A.

Akira Isogai
Graduate School of Agricultural and Life Science, University of Tokyo, Tokyo, Japan

I. INTRODUCTION

This chapter represents a summary review and an update of an earlier discussion of the phenomenology of cellulose, together with an overview of recent developments in the chemistry of cellulose. Rather than attempting to integrate the discussions, they will be presented in two separate sections. Part A, by R.H. Atalla, deals with the states of aggregation of celluloses and key structural issues, particularly those with questions of structure still outstanding. Part B, by A. Isogai, presents an overview of recent developments in the chemistry of cellulose, both basic and applied. To minimize the possibility of confusion, the references and figures are numbered consecutively and separately for each of the sections.

Part A

Spectroscopic Characterization

In Part A, we will be concerned with delineating the frontiers of our understanding of cellulose, particularly with respect to its native forms. The presentation is also relevant to the industrial utilization of cellulose, because it addresses the nature of the native forms of many of the feedstocks used, as well as the effects of processes of isolation on structure and reactivity. The evolution of the historical perspective is included in an earlier report [1] and in references cited therein.

II. STRUCTURES

The beginning of the last three decades of studies on the structure of cellulose was marked by the reintroduction of unit cell models based on parallel alignment of the cellulose molecular chains [2,3], not unlike those abandoned by Meyer and Misch [4] in the 1930s, but also incorporating bending of the glycosidic linkage to allow the intramolecular hydrogen bond, as suggested by Hermans [5]. The new models were not consistent with each other, however, apart from the fact that both were based on parallel alignment of the cellulose chains. As French [6] pointed out, they were also not strongly preferred over an antiparallel structure. In the analysis by French [6], it was recognized that the source of the inconsistency was not so much that the different laboratories were using different computational approaches as it was that the different diffractometric data sets were gathered from different samples and represented different intensities for the same reflections. All of these studies were undertaken before the variability of the crystalline forms of native celluloses was revealed through the high-resolution solid-state ^{13}C NMR investigations.

The new crystallographic models also remained in question because the analyses on which they were based incorporated a level of symmetry in the unit cell that was inconsistent with some of the diffractometeric data. Some of the reflections that are consistently observed in electron diffraction patterns and are disallowed by the selection

Report Documentation Page

Form Approved
OMB No. 0704-0188

1. REPORT DATE	2. REPORT TYPE	3. DATES COVERED
2005	**N/A**	**-**

4. TITLE AND SUBTITLE	5a. CONTRACT NUMBER
Recent Development in Spectroscopic and Chemical Characterization of Cellulose	5b. GRANT NUMBER
	5c. PROGRAM ELEMENT NUMBER
6. AUTHOR(S)	5d. PROJECT NUMBER
	5e. TASK NUMBER
	5f. WORK UNIT NUMBER
7. PERFORMING ORGANIZATION NAME(S) AND ADDRESS(ES) **USDA Forest Service Forest Products Lab One Gifford Pinchot Drive Madison WI, 53726-2398**	8. PERFORMING ORGANIZATION REPORT NUMBER
9. SPONSORING/MONITORING AGENCY NAME(S) AND ADDRESS(ES)	10. SPONSOR/MONITOR'S ACRONYM(S)
	11. SPONSOR/MONITOR'S REPORT NUMBER(S)

12. DISTRIBUTION/AVAILABILITY STATEMENT
Approved for public release, distribution unlimited

13. SUPPLEMENTARY NOTES

14. ABSTRACT

15. SUBJECT TERMS

16. SECURITY CLASSIFICATION OF:			17. LIMITATION OF ABSTRACT	18. NUMBER OF PAGES	19a. NAME OF RESPONSIBLE PERSON
a. REPORT	b. ABSTRACT	c. THIS PAGE			
unclassified	**unclassified**	**unclassified**	**UU**	**37**	

Standard Form 298 (Rev. 8-98)
Prescribed by ANSI Std Z39-18

rules for the space group $P2_1$ [3] were ignored in these crystallographic analyses. In addition to the disallowed reflections in the electron diffraction patterns that placed the crystallographic models in question, new spectral evidence was developed pointing to the need for further refinement of the structural models, particularly for native celluloses. The models derived from the crystallographic studies could not rationalize many features of the spectral data known to be quite sensitive to structural variations.

On the other hand, electron microscopic studies based on new staining techniques, specific to the reducing end groups of the polysaccharides, confirmed the parallel alignment of molecular chains within the microfibrils in native celluloses. These findings were further confirmed by the manifestation, at the electron microscopic level, of the action of cellulases specific to the nonreducing end group; they were clearly active at only one end of each microfibril. The remaining questions at the time, therefore, were concerned with the degree to which the symmetry of space group $P2_1$ is consistent with the other structure-sensitive observations.

It is well to revisit the issue of levels of structure at this point and clarify the levels at which the different investigative methods are most sensitive. The crystallographic models, which represent coordinates of the atoms in the unit cell, represent the most complete possible specification of structure because they include primary, secondary, and tertiary structures. And indeed, crystallographic studies of the monosaccharides and of related structures provide the basis for considerable information concerning bond lengths and bond angles, as well as conformations in saccharide structures. However, for polymeric systems, the diffractometric data are far more limited than for a single crystal of a low-molecular weight compound, so that diffraction data from a polymer must be complemented by information from other structure-sensitive methods. An acceptable model must rationalize not only the diffractometric data, which for cellulose are quite limited in comparison to the number of coordinates that must be specified in a definition of the unit cell, but it must also be such that they can be reconciled with information derived from other experimental measurements known to be sensitive to different levels of structure.

The new spectral evidence that must be rationalized by any acceptable structure came from two methodologies that are most sensitive to structure at the secondary and tertiary levels. These are Raman spectroscopy and solid-state ^{13}C nuclear magnetic resonance (NMR) spectroscopy, both of which were applied to cellulosic samples for the first time during the mid-1970s. The exploration of spectra measurable by these two methods can provide significant information concerning both secondary and tertiary structures in the solid state. Because the spectral features observed are also sensitive to molecular environment, they are influenced by the degree of symmetry of the aggregated state. Hence they provide another avenue for exploration of the applicability of the symmetry of space group $P2_1$ to the structures of the solid state.

III. NEW SPECTROSCOPIC METHODS.

A. Raman Spectroscopy

Both Raman and infrared spectroscopy provide information about chemical functionality, molecular conformation, and hydrogen bonding. Raman spectroscopy, however, has 'some important advantages in the study of biological materials. The key advantage arises from the different bases for activity of molecular vibrations in the Raman and infrared spectra. That is, whereas activity in the infrared region requires finite transition moments involving the permanent dipoles of the bonds undergoing vibrations, activity in the Raman spectrum requires finite transition moments involving the polarizabilities of the bonds. Thus in infrared spectroscopy, the exchange of energy between the molecules and the exciting field is dependent on the presence of an oscillating permanent dipole. In Raman spectroscopy, in contrast, the exciting field induces a dipole moment in the molecule and the induced moment then becomes the basis for exchange of energy with the exciting field. It is useful in this context to view bonds in terms of Pauling's classification [7] along a scale between the two extremes of polar and covalent. Bonds that are highly polar and possess relatively high dipole moments and reduced polarizabilities tend, when they undergo vibrational transitions, to result in bands that are intense in the infrared and relatively weak in Raman spectra. Conversely, bonds that are primarily covalent in character and have relatively low permanent dipoles and high polarizabilities generally result in bands that are intense in the Raman spectra, but are relatively weak in the infrared. This is perhaps best illustrated by the fact that O_2 and N_2, which are homonuclear and without permanent dipoles, have very intense Raman spectra although they are inactive in infrared absorption, while H_2O, with a high permanent dipole moment, is a very strong absorber in the infrared but a very weak Raman scatterer. With respect to cellulose, the O–H groups of cellulose and those of adsorbed water are dominant in many of the spectral features in infrared spectra. In contrast, the skeletal C–C bonds and the C–H bonds dominate the Raman spectra. A further simplification in the Raman spectra results from the circumstance that the selection rules forbidding activity of overtone and combination bands are more rigidly adhered to than is the case in infrared spectra so that the bands observed in Raman spectra are usually confined to the fundamental modes of the molecules under investigation[8].

In the context of studies on the structure of cellulose, the key advantage of Raman spectroscopy is the degree of its sensitivity to the skeletal vibrations of the cellulose molecule, with the mode of packing in the lattice having only secondary effects. This sensitivity is a consequence of the reality that most of the skeletal bonds are C–C bonds and C–O bonds, both of which have relatively high polarizabilities and, hence, high Raman scattering coefficients. The minimal contribution of packing effects arises from the low Raman scattering coefficients of the highly polar O–H

groups, which are the functionalities that are most directly involved in intermolecular associations. The result is that intramolecular variations such as changes in internal coordinates have a significantly greater influence on the Raman spectra than do variations in intermolecular associations.

Finally and very significantly, as the studies of the celluloses progressed, it became clear that the most dramatic differences between the spectra associated with different states of aggregation of cellulose occurred in the region between 200 and 700 cm^{-1}, which is generally inaccessible with most infrared spectrometers.

These considerations were paramount in the first detailed examination and comparison of the Raman spectra of celluloses I and II [9]; the spectra are shown in Fig. 1. It was concluded that the differences between the spectra, particularly in the low-frequency region, could not be accounted for in terms of chains possessing the same conformation, but packed in different ways in the different lattices. As noted earlier, that had become the accepted rationalization of the differences between celluloses I and II, as developed from diffractometric studies of these two most common allomorphs. The analyses of the Raman spectra led to the proposal that two different stable conformations of the cellulose chains occur in the different allomorphs.

To establish a basis for assessing the differences between celluloses I and II, Atalla and coworkers undertook an extensive series of studies of model compounds of increasing complexity [IO–181. The model systems investigated included the 1,5-anhydropentitiols, the pentitols and erythritol, the pentoses, the inositols, the hexoses, and the cellobiose. The studies included comprehensive normal coordinate analyses of the molecular vibrations of each of the groups of model compounds based on complementary infrared and Raman spectra. The objective of these analyses was to establish the degree to which the different classes of vibrational motions contribute to the spectral features in the different regions of the spectrum. Such a comprehensive approach was necessary because the skeletal bond systems occurring in the structures of carbohydrates are predominantly made up of C–C and C–O bonds, which possess similar reduced masses and vibrational force constants and, hence, have very similar vibrational frequencies. In consequence, a high degree of coupling occurs between the vibrations, with the result that very few of the vibrational modes are localized within specific bonds or functional groups. Thus, the traditional group frequency approach common in the assignment of infrared and Raman spectra is of very limited use, except in the case of vibrations localized in the bonds of hydrogen atoms bonded to much heavier atoms such as O or C. On the other hand, the normal coordinate analyses allow identification of the degree to which the vibrations of each of the internal coordinates contributes to each of the observed bands. Because the coupling of the vibrations is very sensitive to changes in the bond angles and in the dihedral angles associated with the bonds the vibrations of which are coupled, the normal coordinate analyses allow a detailed and systematic exploration of the effects of differences in skeletal conformations on the bands associated with particular vibrations.

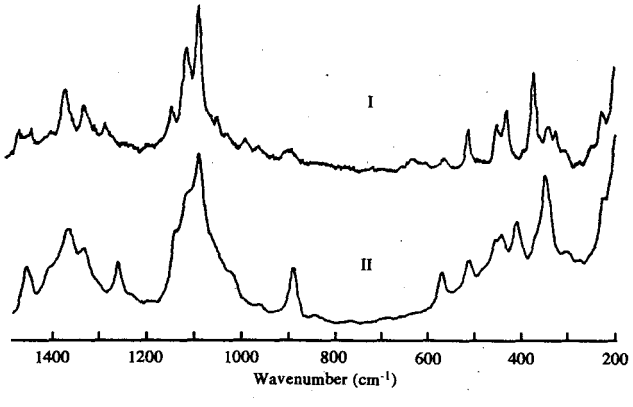

Figure 1 Raman spectra of high-crystallinity celluloses I and II.

With respect to the question concerning the conformations of celluloses I and II, it is useful to first consider some of the pertinent information developed from the normal coordinate analyses, particularly with respect to the classes of molecular motions associated. with the different spectral features. The region below 1500 cm^{-1} was the primary focus of the early exploration because the intense bands clustered at about 2900 cm^{-1} can be identified with the C–H stretching vibrations and the region beyond 3000 cm^{-1} is clearly associated with the O–H stretching vibrations. In addition to the C–H and O–H stretching vibrations, the internal deformation of the methylene group on C6 is the only vibration that closely approximates a group or local mode in the usual sense implicit in discussions of assignments of vibrational spectra; the HCH bending vibration usually occurs above 1450 cm^{-1}. In all other bands at frequencies below 1450 cm^{-1}, the normal coordinate analysis indicated that the vibrations are so highly coupled that, in most instances, no single internal coordinate contributes more than 20% of the potential energy change associated with any particular frequency, although in a few instances contributions were as high as 40%. Thus, as noted above, the traditional group frequency approach to assignment of vibrational spectra, which is based on the concept of local modes, is generally not applicable in this region in the spectra of saccharides. Instead, it is necessary to focus on the classes of internal motions that are associated with the different frequency ranges and to interpret the spectra in terms of the influence that variations in the internal coordinates can have on the coupling between different types of vibrational deformations.

For analysis of the spectra of celluloses, it is possible to classify the groups of features in the different spectral regions in terms of the types of internal deformations that make their maximum contributions to bands in those regions. The bands between 1200 and 1450 cm^{-1} are attributable to modes involving considerable coupling

between methine bending, methylene rocking and wagging, and COH in-plane bending motions; these are angle bending coordinates involving one bond to a hydrogen atom and the other to a heavy atom. Significant contributions from ring stretching begin below 1200 cm^{-1} and these modes, together with C–O stretching motions, dominate between 950 and 1150 cm^{-1}. Below 950 cm^{-1}, angle bending coordinates involving heavy atoms only (i.e., CCC, COC, OCC, OCO) begin to contribute, although ring and C–O stretches and the external bending modes of the methylene group may be major components as well. The region between 400 and 700 cm^{-1} is dominated by the heavy atom bending, both C–O and ring modes, although some ring stretching coordinates still make minor contributions. In some instances O–H out-of-plane bending motions may make minor contributions in this region as well. Between 300 and 400 cm^{-1}, the ring torsions make some contributions, and below 300 cm^{-1}, they generally dominate.

In addition to the above generalized categorization concerning modes that occur in one or another of the model compound systems used in the normal coordinate analyses, the spectrum of cellulose will have contributions because of modes centered at the glycosidic linkage. Computations based on the cellodextrins indicate that these modes are. strongly coupled with modes involving similar coordinates in the adjacent anhydroglucose rings. The contributions of the different classes of internal coordinates to the different bands are presented in greater detail elsewhere [19].

As noted above and shown in Fig. 1, differences between the Raman spectra of celluloses I and II are quite significant particularly in the region of the skeletal bending modes of vibration. In the region above 800 cm^{-1}, the differences are most obvious with respect to the relative intensities of the bands and the broadening of some of the bands upon conversion from cellulose I to cellulose II. In the region below 700 cm^{-1}, in contrast, the main features are quite different in the two spectra; these differences are even more evident in the spectra of single fibers, which will be presented later.

In the analyses of the spectra of model compounds, changes of the magnitude indicated in Fig. 1 were exclusively associated with the occurrence of differences in conformations. It seemed very probable therefore that the differences between the spectra of celluloses I and II reflect a change in molecular conformation accompanying the transition from one form to the other. As the basic ring structure is not expected to change [19], it would appear that variations in the dihedral angles at the glycosidic linkages provide the only opportunity for conformational differences. Because of the controversy surrounding similar conclusions based on crystallographic studies carried out in the early 1960s [21, 22], a number of experimental and theoretical avenues for validating this interpretation were pursued.

The first consideration was whether a multiplicity of stable conformations is consistent with the results of conformational energy calculations that were available at the time [20, 23]. In both studies, the potential energy surfaces were found to possess multiple minima. When the additional constraint of a repeat length of approximately 0.515 nm per anhydroglucose unit was added, two minima representing both left-handed and right-handed departures from the twofold helix appeared to be likely loci of the stable conformations. It was noted in this context that these two minima were close to the positions of the dihedral angles of the glycosidic linkages in cellobiose and methyl β cellobioside, respectively, as these were determined from crystallographic studies [24, 25].

Next, inquiry was made into the degree to which changes in the dihedral angles about the bonds in the glycosidic linkage could influence the modes of vibration responsible for the spectral features in the different regions of the spectra. Two approaches were adopted for this purpose. The first was based on examining the Raman spectra of polysaccharide polymers and oligomers that were known to occur in different conformations. The second was a theoretical one based on an adaptation of the matrix perturbation treatment used by Wilson et al. [26] to discuss the effects of isotopic substitution on infrared and Raman spectra.

The polysaccharide systems chosen for investigation were among those most closely related to cellulose in the sense that they are the α-1,4-linked polymers and oligomers of anhydroglucose. They included amylose and two of its cyclic oligomers, with primary emphasis on the latter, the α- and β-Schardinger dextrins, often also known as cyclohexa- and cyclohepta-amylose. The structures of the two oligomers differ in that the values of the dihedral angles about the bonds of the glycosidic linkages have to change to accommodate the different number of monomer units. Comparison of the Raman spectra of the cyclic dextrins showed that the differences between them were quite minor in the regions above 800 cm^{-1}, but they were quite significant in the lower frequency region dominated by the skeletal bending and torsional modes. The differences were similar in kind and distribution to the differences between celluloses I and II. It was also noted that in earlier studies of the Raman spectra of amylose [27], it had been observed that forms V_a and V_h, which are very similar in conformation but had different levels of hydration, had almost identical spectra. In contrast, form B, which is known to have a distinctly different helix period, was found to have a spectrum that differs from those of forms V_a and V_h in a manner approximating the differences between the two cyclic oligodextrins. Taken together, the observations of the Raman spectra of the amyloses support the interpretation of the differences between the Raman spectra of celluloses I and II as pointing to differences in the chain conformations localized at the glycosidic linkages.

In the theoretical analysis, the method of Wilson et al. [26] was adapted to explore the consequences of variations in the dihedral angles about the bonds in the glycosidic linkage; this approach is discussed in greater detail elsewhere [1]. These considerations led to the conclusion that skeletal bending and torsional modes are altered to a greater degree than the skeletal stretching modes when the dihedral angles associated with the glycosidic linkage undergo variations. When translated to spectral features

in the Raman spectra, these observations point to major differences in the low frequency region below 700 cm^{-1}, and minor ones in the fingerprint region between 900 and 1500 cm^{-1}. These are indeed precisely the types of differences observed in comparisons of the spectra of celluloses I and II.

One final consideration that was addressed is the possibility that rotations of the primary alcohol group at C6 could account for the spectral differences seen in the spectra of celluloses I and II and in the spectra of the amyloses. The normal coordinate analyses of the hexoses showed that rotations about the C5–C6 bond can result in minor variations in the region below 600 cm^{-1}, but that the major impact of such rotations is expected in the spectral region above 700 cm^{-1} [16, 17]. With all of the above considerations in mind, it became clear that the only plausible rationalization of the differences between the Raman spectra of celluloses I and II had to be based on the possibility that differences between the skeletal conformations were the key.

The first effort to rationalize differences in conformation was based on the results of the conformational energy mappings that were available at the time [20, 23]. The key points derived from those analyses, which have been confirmed by more recent studies [28, 29], were that the two energy minima associated with variations in the dihedral angles of the glycosidic linkage correspond to relatively small left-handed and right-handed departures from glycosidic linkage conformations that are consistent with twofold helical symmetry. The minima also represented values of the dihedral angles that were very similar to those reported for cellobiose and methyl β cellobioside on the basis of crystallographic analyses [24, 25]. The relationship between the different conformations is represented in Fig. 2, which was adapted by Atalla [30] from a diagram first presented by Rees and Skerret [20]. It is a ψ/ϕ map

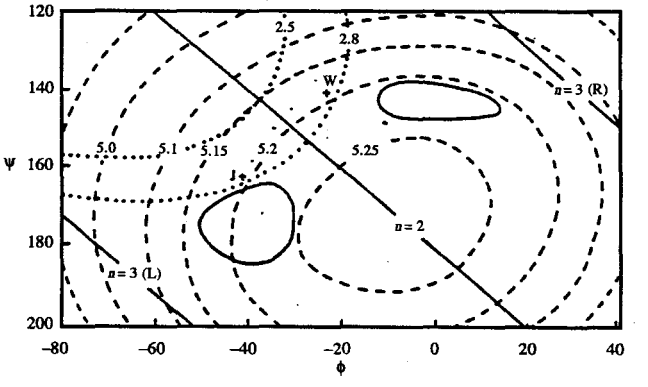

Figure 2 ψ/ϕ map (- - - - –) loci of structures with constant anhydroglucose repeat periods: (· · · · · ·) loci of structures of constant intramolecular hydrogen bond (O–O) distances; (_____) contours of potential energy minima based on nonbonded interactions in cellobiose; W, β-methylcellobiose, $n = 2$, the twofold helix line; $n = 3$ the threefold helix lines; (R) right-handed, (L) left-handed. The Meyer–Misch structure is at $\psi = 180$, $\phi = 0$.

presenting different categories of information concerning the conformation of the anhydrocellobiose unit as a function of the values of the two dihedral angles about the bonds in the glycosidic linkage. ψ is defined as the dihedral angle about the bond between C4 and the glycosidic linkage oxygen and ϕ as the dihedral angle about the bond between C1 and the glycosidic linkage oxygen. The parallel lines indicated by $n = 3$(L), 2, and 3(R) represent values of the dihedral angles that are consistent with a left-handed threefold helical conformation, a twofold helical conformation, and a right-handed threefold helical conformation, respectively; a twofold helical conformation inherently does not have a handedness to it. The dashed contours represent conformations that have the indicated repeat period per anhydroglucose unit; the innermost represents a period of 5.25 A corresponding to 10.5 A per anhydrocellobiose unit. The two dotted lines indicate conformations corresponding to values of 2.5 and 2.8 A for the distance between the two oxygen atoms anchoring the intramolecular hydrogen bond between the C3 hydroxyl group of one anhydroglucose unit and the ring oxygen of the adjacent unit; the values bracket the range wherein hydrogen bonds are regarded as strong. The two domains defined by solid lines on either side of the twofold helix line ($n = 2$) represent the potential energy minima calculated by Rees and Skerret for the different conformations of cellobiose. Finally, the points marked by J and W represent the structures of cellobiose determined by Chu and Jeffries [24] and the structure of methyl β cellobioside determined by Ham and Williams [25]. The key point to be kept in mind in relation to this diagram is that structures along the twofold helix line and with a repeat period of 10.3 Å per anhydrocellobiose unit possess an unacceptable degree of overlap between the van der Waals radii of the protons on either side of the glycosidic linkage.

Consideration of these issues together with the results of the Raman spectral observations led to exploration of the possibility that small departures from the twofold helix structures may be small enough that the conformation was still approximated by a twofold helix. Some plausible alternatives were explored. One was motivated by the comparisons of the Raman spectra of cellulose II and of cellobiose in the O–H stretching region [30]. The latter showed a single sharp band superimposed on a broader background, and the band was identified with the O–H stretching vibration of the isolated intramolecular hydrogen bond revealed in the crystal structure [24]; it occurs between the hydroxyl group on C3 of the reducing anhydroglucose unit and the ring oxygen of the nonreducing unit. The spectrum of cellulose II revealed two such sharp bands in the same region; similar bands were observed in the spectra of the cello-oligodextrins [18]. As the frequency at which such bands occur is very sensitive to the distance between the oxygen atoms anchoring the hydrogen bond, it appeared that the structure of cellulose II must incorporate intramolecular hydrogen bonds with two distinct values of the O–O distance. This led to the proposal that successive units in the structure are not equivalent, and that, as a consequence, alternating glycosidic linkages have different sets of dihedral angles defining their coor-

dinates [30]. Thus, the dimeric anhydrocellobiose was regarded as the repeat unit of physical structure rather than the anhydroglucose unit. These conclusions, based on the Raman spectra in the O–H region, were confirmed when the solid-state ^{13}C NMR spectra became available [31] as splittings were observed in the resonances associated with C1 and C4, which anchor the glycosidic linkage. The occurrence of these splittings is indicative of the presence of nonequivalent glycosidic linkages within the structure; the NMR spectra will be considered in greater detail in a subsequent section.

Upon further reflection, it was recognized that when alternating glycosidic linkages are admitted as an option, and when anhydrocellobiose is viewed as the repeat unit of structure, the alternating glycosidic linkages need not have the same sense of departure from the twofold helix. That is, it was now possible to consider structures wherein the nonequivalent glycosidic linkages are alternating left-handed and right-handed departures from the twofold helix. Such structures would be ribbonlike and could appear to approximate the twofold helix. The proposal incorporating the alternating glycosidic linkage has the advantage that it can be reconciled with much of the diffractometeric data. If the departure from twofold helical symmetry is relatively small, it may account for the weakness of the reflections that are disallowed by the selection rules of space group $P2_1$.

Based on the considerations outlined, the model that was adopted as a basis for continuing explorations of the spectra of cellulose was based on the proposal that the glycosidic linkages alternated between small left-handed and right-handed departures from the twofold helical conformation. Thus, differencesbetween the conformations of celluloses I and II now had to be understood in terms of differences in the internal organization of the anhydrocellobiose units that were the basic units of structure [32, 33].

In search of a rationalization of the changes in the internal organization of the cellobiose unit associated with the transition from cellulose I to cellulose II, Atalla drew on an analogy with the structures of cellobiose and methyl β cellobioside, which are represented in Fig. 3. The methyl β cellobioside, which has values of the dihedral angles corresponding to a right-handed departure from the twofold helix, also has a bifurcated intramolecular hydrogen bond in which the proton from the C3 hydroxyl group appears to be located between the ring oxygen and the primary alcohol oxygen at C6 of the adjacent unit. This bifurcation is in part responsible for the absence of a sharp OH band in the OH region of the spectrum of the methyl β cellobioside. Atalla suggested that such bifurcated intramolecular hydrogen bonds may occur in connection with every other glycosidic linkage in a molecule of native cellulose; these bifurcated hydrogen bonds would be associated with those glycosidic linkages that have values of the dihedral angles representing right-handed departures from the twofold helix in a manner not unlike those in methyl β cellobioside. The action of mercerizing agents was seen as resulting in the disruption of the bifurcated OH bonds, thus, allowing the glycosidic linkages to relax to slightly greater departure from the twofold helix [22, 23]. Such an

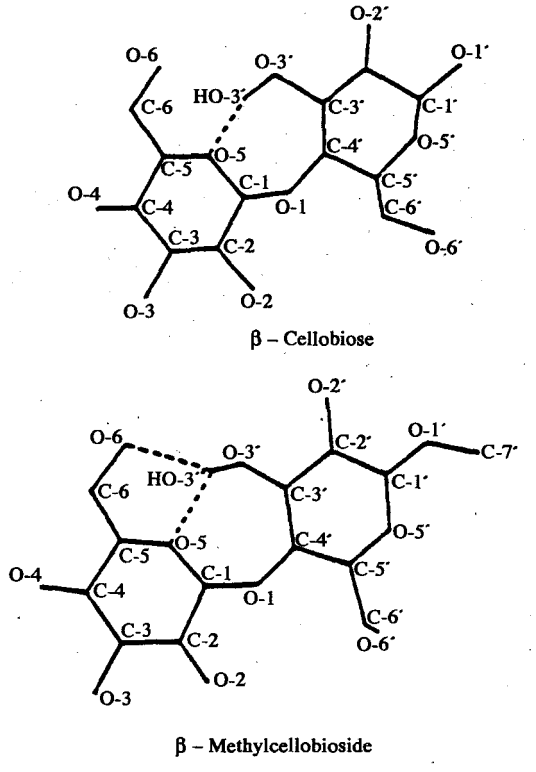

Figure 3 Structure of β-cellobiose and β-methylcellobioside.

explanation would also be consistent with the observation that the two HCH bending bands in the Raman spectra of native celluloses collapse into a single band upon mercerization, suggesting a nonequivalence of the two primary alcohol groups in native cellulose and a shift closer to equivalence upon mercerization. It is also consistent with the greater splitting of the resonances associated with C1 and C4 seen in the solid-state ^{13}C NMR spectra of cellulose II to be discussed in the following section. While the evidence supporting this proposal is strong, it is not conclusive and, thus, awaits further confirmation. Atalla also introduced the terms k_I and k_{II} to designate the conformations corresponding to celluloses I and II; the term k_0 was introduced to describe cellulose in a disordered state [34.].

B. Solid-state ^{13}C NMR Spectra and the Two Forms of Native Cellulose I, and I,

Although applied to cellulose later than Raman spectroscopy, high-resolution solid-state ^{13}C NMR has provided perhaps the most significant new insights regarding the structures of cellulose, particularly in its native state. The development of high-resolution solid-state NMR spectroscopy and its application to polymeric materials grew from complementary application of a number of procedures that had been developed in NMR spectroscopy. The first is proton carbon cross-polarization (CP) that is used to enhance sensitivity to the low abundance ^{13}C nucleus. This was combined with high-power proton decoupling to

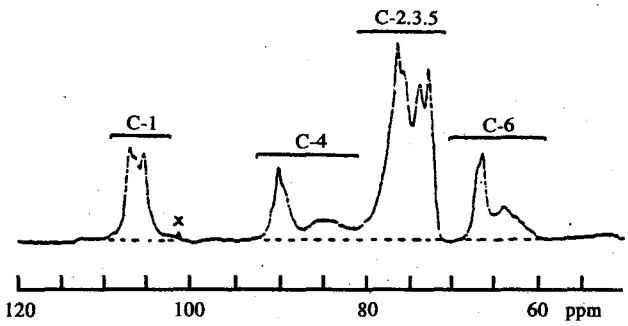

Figure 4 ^{13}C CP-MAS spectrum of cotton linters. The horizontal bars indicate the spectral ranges of the corresponding carbon sites in the anhydroglucose monomer unit of cellulose.

eliminate the strong dipolar interaction between the ^{13}C nuclei and neighboring protons. Finally, the angular dependence of the chemical shift, or chemical shift anisotropy, is overcome by spinning the sample about an axis at a special angle to the direction of the magnetic field, commonly referred to as the magic angle, the procedure denoted by (MAS). The combined application of these procedures, usually designated by (CP/MAS), results in the acquisition of spectra that contain isotropic chemical shift information analogous to that obtained from liquid-state ^{13}C NMR with proton decoupling.

In summary, the most important characteristic of the spectra acquired using the (CP/MAS) ^{13}C NMR technique is that, if they are acquired under optimal conditions, they can have sufficient resolution so that chemically equivalent carbons occurring in magnetically nonequivalent sites can be distinguished. In the present context, the corresponding carbons in different anhydroglucose units would be regarded as chemically equivalent. If they are not also symmetrically equivalent, that is, if they occur in different environments or if the anhydroglucose rings possess different conformations, within the rings, or at the glycosidic linkage, or at the primary alcohol group, the carbons will not have magnetically equivalent environments and will, therefore, result in distinctive resonances in the NMR spectrum. The fundamental challenge in the application of this method is to achieve a level of resolution sufficient to distinguish nonequivalences between chemically equivalent carbons, because the magnetic nonequivalence can result in variations in the chemical shift that are small relative to the shifts determined by the primary chemical bonding pattern.

Another important feature of the (CP/MAS) ^{13}C NMR technique is that, for a system such as cellulose, which consists of rather rigid hydrogen-bonded molecules and in which all carbons have directly bonded protons, the relative intensities of the resonances are expected to correspond to the proportion of the particular carbons giving rise to them. Thus, the intensities arising from each of the six carbons in the anhydroglucose ring are expected to be equal. This is an important characteristic that is central to the analysis and interpretation of the information contained within the spectra.

The first applications of the new technique to cellulose [31, 35] demonstrated resolution of multiple resonances for some of the chemically equivalent carbons in the anhydroglucose units. It became clear that rationalization of the spectra that were observed would provide valuable additional information concerning the structure of the celluloses investigated, The first step in such a rationalization was the assignment of the resonances that appear in the spectra. The assignments, which have been discussed in a number of reports [31, 35–40], were based on comparisons with solution spectra of cello-oligosaccharides and of a low-DP cellulose [41]. They are indicated in Fig. 4, which shows a spectrum of cotton linters [42]. Beginning at the upfield part of the spectrum, the region between 60 and 70 ppm is assigned to C6 of the primary alcohol group. The next cluster of resonances, between 70 and 81 ppm, is attributed to C2, C3, and C5, the ring carbons other than those anchoring the glycosidic linkage. The region between 81 and 93 ppm is associated with C4, and that between 102 and 108 ppm with C1, the anomeric carbon.

In one of the first reports on the application of the technique to studies of different celluloses, the splittings of the resonances of C4 and C1 in the spectrum of cellulose II (Fig. 5) were regarded as confirmation of the occurrence of nonequivalent glycosidic linkages that had earlier been proposed on the basis of the comparison of the Raman spectra of cellulose II and of cellobiose in the O–H stretching region [31]. These splittings were also observed in the CP/MAS spectra of the cello-oligodextrins, which crystallize in a lattice very similar to that of cellulose II. In that context the splittings were attributed to the occurrence of

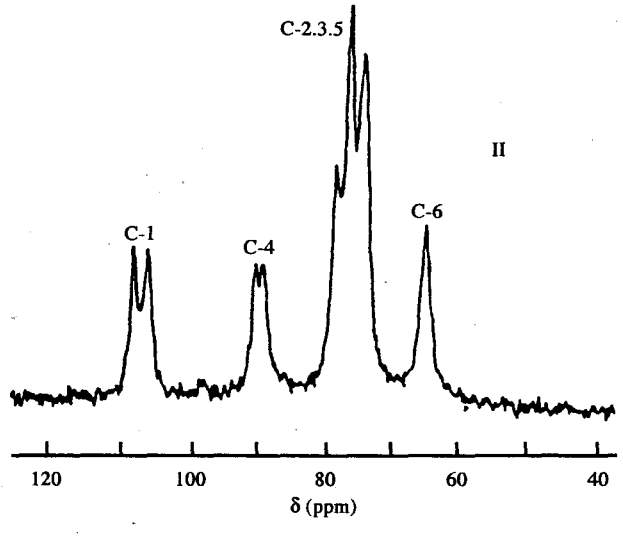

Figure 5 CP/MAS ^{13}C spectrum of high-crystallinity cellulose II recorded at relatively low resolution. Chemical shifts are shown in parts per million relative to Me_4Si. Assignment of the C-1, C-4, and C-6 resonances are based on pertinent liquid-state spectra.

nonequivalent cellulose molecules in the same unit cell [38]. However, such an interpretation leaves open the question as to why the resonances for carbons 2, 3, and 5, do not display similar splittings. If the splittings were indeed due to nonequivalent molecules, it would be anticipated that those carbons nearest to the boundaries of the molecule would be the most affected. The carbons anchoring the glycosidic linkage, that is C1 and C4, are the ones most removed from adjacent molecules, yet they also display the greatest splittings.

Interpretation of the spectra of native celluloses presented an even more challenging task. In the spectrum of cotton linters (Fig. 4), the two resonance regions associated with C6 and C4 include sharper resonances overlapping broader upfield wings. After excluding the possibility that the broader wings could arise entirely from molecular mobility [35, 36], the wings were attributed to cellulose chains in two categories of environment. The first includes all chains located at the surfaces of cellulose microfibrils, which, because of their occurrence at the boundary, are less constrained with respect to the conformations they can adopt. The surfaces are regarded as regions of limited two-dimensional order. The importance of this category of order had earlier been demonstrated in a study of different native celluloses undertaken by Earl and VanderHart [36]. The celluloses had natural fibril diameters varying between 3.5 and 20 nm, and it was shown that the areas of the upfield wings of C4 and C6 declined as the surface-to-volume ratio declined. The second category of environments contributing to the upfield wings is that of chains in regions within which the incoherence of order is not limited to two dimensions. Here, the dispersion of the frequencies at which resonances occur may arise from conformational differences, variations in bond geometries, changes in hydrogen bonding patterns, and nonuniformities in neighboring chain environments. These possibilities arise because in such regions the molecular chains are free to adopt a wider range of conformations than the ordering in a crystal lattice or its boundaries would allow.

Although the obvious upfield wings of the C4 and C6 resonances are the most direct evidence for the cellulose chains in less-ordered environments, it is expected that the chains in these environments make similar contributions to the resonance regions associated with the other carbons. In the region of C1, the contribution appears to be primarily underneath the sharper resonances, although a small component appears to extend toward 104 ppm. Similarly, it is expected that the contribution from chains in the less-ordered environments underlie the sharper resonances of the C2, C3, and C5 cluster.

The relative contributions of the two categories of environment to the intensities of the upfield wings were assessed in a careful analysis of the C4 wing [42]. It was demonstrated that part of the wing could be correlated with the range of the C4 resonance in amorphous cellulose prepared by ball milling. It was therefore assigned to cellulose chains occurring in the second type of environment, that is, domains wherein the incoherence of order is extended in all three dimensions. The other part of the wing was attributed to chains at the surfaces of the fibrils and, on the basis of these comparisons, it was concluded that approximately 50% of the wing is contributed by cellulose chains in each of the two types of less-ordered environments described in the preceding paragraph. Although the upfield wing of C4 is the basis of this allocation of intensities, it can be assumed that the relative contributions are similar for the upfield wing of C6 and for the component that appears to underlie the sharper resonances at C1. It is also expected that these domains contribute to the total intensity of the C2, C3, and C5 cluster between 70 and 81 ppm.

The sharper resonances in the C6 and C4 regions, centered at 66 and 90 ppm, respectively, each appear to consist of more than one resonance line, although the resolution is not sufficient to distinguish the components well. The C6 resonance seems to include at least two components while the C4 resonance appears to include three closely spaced component lines. These multiplicities were interpreted as arising from carbons in cellulose molecules within the interior of crystalline domains and are therefore taken as evidence of the occurrence of chemically equivalent carbons in different magnetic environments within the crystalline domains.

The region between 102 and 108 ppm, attributed to C1, also reveals multiplicity and sharp resonance features. Here, however, the shoulder is very limited. It appears that the resonances associated with the two categories of disordered domains described above lie underneath the sharp resonances associated with the interior of the crystalline domains. It can be concluded that, in most instances, the dispersion of frequencies associated with the disorder is small relative to the shift associated with the character of the anomeric carbon C1, while that is not the case for the shifts associated with C4 and C6. One possible rationalization may be that, because of the anomeric effect, the internal coordinates surrounding C1 are much less flexible within the range of possible conformational variations than are the other internal coordinates.

In search of a rationalization of the splittings observed in the sharp resonances, (CP/MAS) ^{13}C NMR spectra of a wide variety of samples of cellulose I were recorded. Some of these are shown in Fig. 6. They include ramie fibers (a), cotton linters (b), hydrocellulose prepared from cotton linters by acid hydrolysis (c), a low-DP regenerated cellulose I (d), cellulose from *Acetobucter xylinum* (e), and cellulose from the cell wall of *Valonia ventricosa* (f), an alga. While similar observations were reported in a number of studies [31, 32, 36-40], their implications with respect to structure were more fully developed in the work of VanderHart and Atalla [42, 43], which provides the basis for the following discussion.

All of the spectra shown in Fig. 6 (A–F) are of celluloses that occur in relatively pure form in their native states and require relatively mild isolation procedures. The most striking feature in these spectra, when viewed together, is the variation in the patterns of the multiplets at C1, C4, and C6. These resonances, which are viewed as arising from chains in the interior of crystalline domains, appear to be unique to the particular celluloses; among the native forms

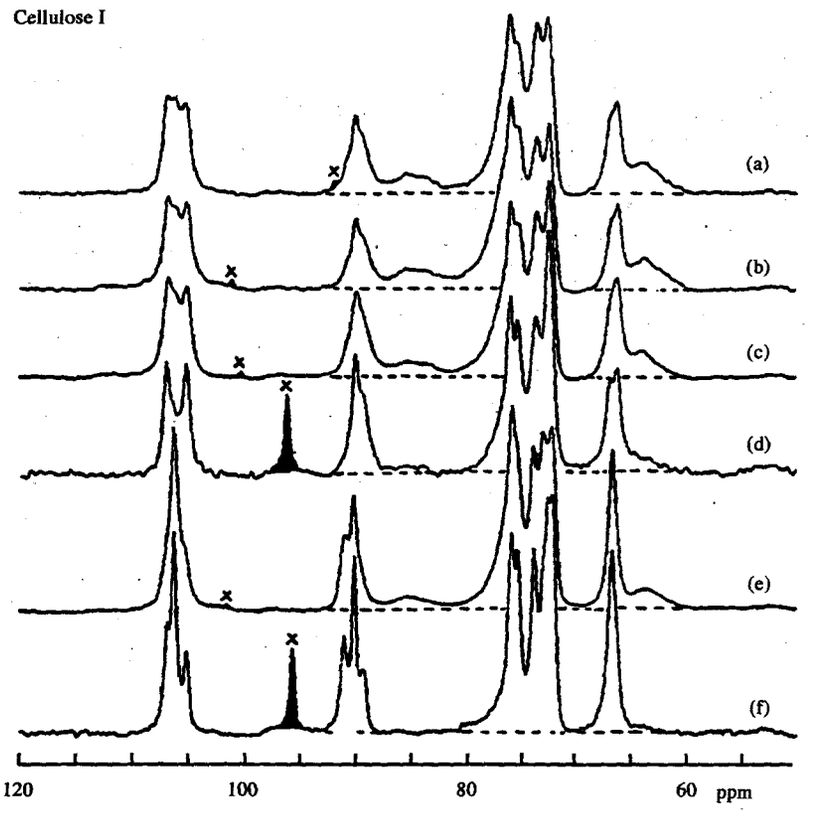

Figure 6 ^{13}C CP-MAS spectra of several cellulose I samples: (a) ramie; (b) cotton linters; (c) hydrocellulose from cotton linters; (d) a low-DP regenerated cellulose I; (e) *Acetobacter xylinum* cellulose; (f) *Valonia renrricosa* cellulose. Note the varied fine structure particularly at C-1 and C-4. Signal-to-noise variation due to limited amount of some samples. In that instance more polyethylene was added so the side band intensity increased. No line broadening or resolution enhancement techniques were applied in the acquisition of the spectra (after VanderHart and Atalla).

they appear to be distinctive of the source species. The first attempt to rationalize the spectra was in terms of information that they might provide concerning the unit cell of the structure of cellulose I. However, it soon became obvious that such a rationalization was not possible because the relative intensities within the multiplets were not constant, nor were they in ratios of small whole numbers as would be the case if the same unit cell prevailed throughout the crystalline domains. The conclusion was that the multiplicities were evidence of site heterogeniety within the crystalline domains and that therefore native celluloses must be composites of more than one crystalline form.

Further rationalization of the spectra required a careful analysis of the mutliplets at C1, C4, and C6, and the variations of the relative intensities of the lines within each multiplet among the spectra of the different celluloses. In addition to excluding a single crystal form on the basis of the considerations noted above, it was also possible to exclude the possibility of three different forms with each contributing a line to the more complex multiplets. Thus, a decomposition of the spectra on the basis of two distinct crystalline forms was pursued. The results of the decomposition are shown as spectra (b) and (c) in Fig. 7, and were designated as the I_α and I_β forms of native cellulose; this designation was chosen in order to avoid the possibility of confusion with the I_A and I_B forms that had earlier been defined in terms of differences in the appearance of the O–H bands in different types of native celluloses [44, 45]. Spectrum (A) was acquired from a high-crystallinity sample of cellulose II and is included so as to distinguish the heterogeniety of crystalline forms occuring in the different forms of cellulose I from the long-known polymorphic variation of the crystallinity of cellulose.

Spectra b and c in Fig. 7 were in fact derived from appropriate linear combinations of the spectra of the low-DP cellulose I (d) and of the *A. xylinum* cellulose (e) in Fig. 6. Although they represent the best approximations to the two forms of cellulose postulated, they cannot be regarded as representative of the pure forms as they do not adequately reflect the component of the cellulose at the surfaces of the crystalline domains. Spectrum 7B does have some intensity in the upfield wings of C4 and C6, but spectrum 7C has very little evidence of such wings. There is very little question, however, that the sharp components of

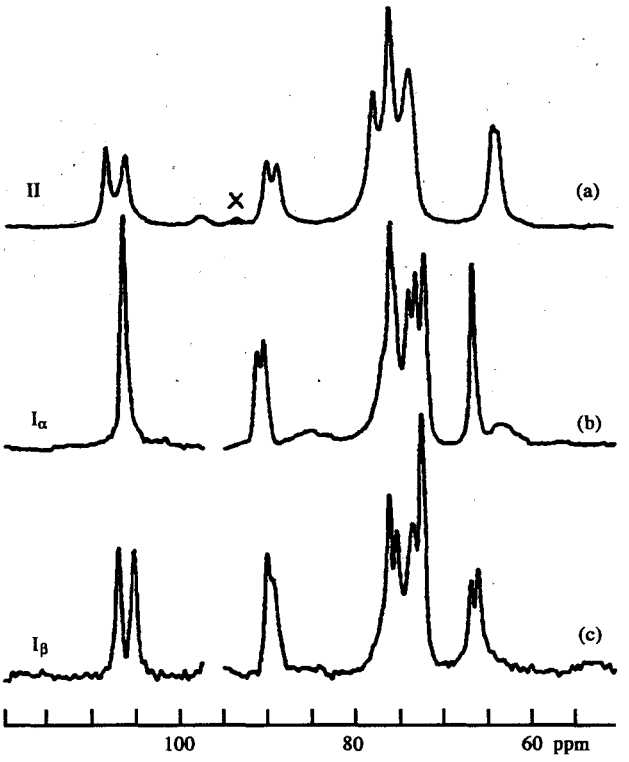

Figure 7 Comparison of the ^{13}C CP-MAS spectrum (a) of a low-DP cellulose II sample and the spectra (b) and (c) corresponding, respectively, to the two proposed crystalline forms of cellulose I, namely I_α and I_β. Spectra (b) and (c) were obtained by taking linear combinations of the low-DP and *Acetobacter* cellulose spectra. Discontinuities in spectra (b) and (c) occur where the polyethylene sidebands would have appeared. The I_α spectrum still contains a significant amount of non-I_α resonances as shown by the visible C-4 and C-6 upfield wings. Multiplicities of the C-1, C-4, and C-6 narrower resonances ought to indicate unit cell inequivalences.

spectra 7B and 7C include the key features in the spectra of the I_α and I_β forms. It is of interest to note here that among the distinct resonances of the I_α form at C1, C4, and C6, only the one at C4 appears to be split, while for the I, form all three resonances associated with these carbons show splitting, with the one at C1 the most pronounced.

In an effort to further validate the proposal that the I_α and I_β forms were the primary constituents of native celluloses, VanderHart and Atalla [46] undertook another extensive study to exclude the possibility that experimental artifacts contributed to the key spectral features assigned to the two forms. A number of possible sources of distinctive spectral features were explored. The first was the question whether surface layers associated with crystalline domains within particular morphological features in the native celluloses could give rise to features other than those of the core crystalline domains. The second was whether variations in the anisotropic bulk magnetic susceptibility associated with different morphologies could contribute distinctive spectral features. Exploration of the spectra of higher plant celluloses with different native morphologies revealed very little difference in the essential features of the spectra, even after the samples had been subjected to acid hydrolysis. Furthermore, it was concluded that the I, component of higher plant celluloses was sufficiently low that some question was raised as to whether it occurs at all in these higher plant celluloses. In this context, it was also concluded that without the I_α component in higher plant celluloses, the lineshapes of the I_β form at C4 could only be reconciled with a unit cell possessing more than four anhydroglucose residues per unit cell.

Attention was then directed to analysis of the spectra of algal celluloses, wherein the I_α component is the dominant one. Relaxation experiments confirmed that the essential spectral features identified with the two crystalline forms of cellulose were characteristic of the core crystalline domains; when measurements were conducted such that magnetization of the surface domains was first allowed to undergo relaxation, very little change in the spectral features was observed. The relaxation experiments suggested that domains consisting of both the I_α and I_β forms have equal average proximity to the surface. One possible interpretation of these observations, that the two forms are very intimately mixed, was ruled out at that time on the basis of hydrolysis experiments the results of which are now in question.

Two groups of modifying experiments were carried out with the algal celluloses. In the first, the algal celluloses were subjected to severe mechanical action in a Waring blender. In the second, the algal celluloses were subjected to acid hydrolysis, in 4 N HC1 for 44 h at 100°C. While the mechanical action resulted in some reduction in the proportion of the I_α form, the acid hydrolysis resulted in a dramatic reduction, sufficient indeed to make the spectra seem like those of the higher plants, except that the resolution of the spectral lines was much enhanced relative to that observed in the spectra of even the purest higher plant celluloses. The samples subjected to hydrolysis, wherein the recovery varied between 12% and 22%, were examined by electron microscopy and shown to have lateral dimensions not unlike those of the original samples. These observations were interpreted to imply that the I_α form is more susceptible to hydrolysis than the I, form. An earlier study of the effect of hydrolysis, under similar conditions but for only 4 h, had been carried out with cellulose from *Rhizoclonium heiroglyphicum* with no discernible effect on the spectra [47]. The difference in duration of the hydrolysis may well have been the key factor. Both of these observations and their interpretations had been presented, however, before it was recognized that exposure of celluloses with relatively high contents of the I_α form to elevated temperatures can result in its conversion to the I_β form [48]. When the possibility that the I_α content of the algal cellulose had been converted to the I_β form is taken into account, the results of the relaxation experiments of VanderHart and Atalla cited above can be reinterpreted as indicating

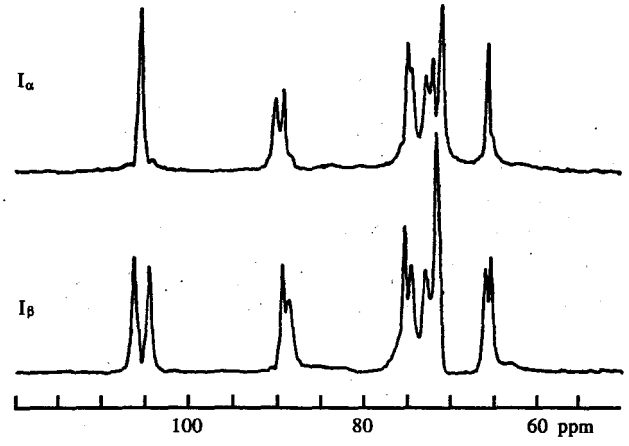

Figure 8 Alternative candidates for the spectra of cellulose I_α (top) and I_β (bottom) derived from linear combinations of the spectra of I_α-rich *Cladophera glomerata,* before and after acid hydrolysis, which resulted in a I_β-rich cellulose.

intimate mixing of the I_α and I_β forms within the crystalline domains of the algal celluloses.

VanderHart and Atalla also took advantage of the spectra derived from the acid hydrolyzed samples of the algal cellulose to generate more highly resolved representative spectra of the I_α and I_β forms. These are shown in Fig. 8, where it is clear that even in the spectrum representative of the I_α form the upfield wings of the C4 and C6 resonances are reduced to a minimum. With the completion of this study by VanderHart and Atalla, most of the questions about the possibility that the spectral features were the results of artifacts were put to rest, and the hypothesis that all native celluloses belong to one or to a combination of these forms was generally accepted.

With the above resolution of the questions concerning the nature of native celluloses in mind, it was possible to classify these celluloses with respect to the relative amounts of the I, and I, forms occurring in the celluloses produced by particular species. It emerged in these early studies that the celluloses from more primitive organisms such as ***V. ventricosa*** and ***A. xylinum*** are predominantly of the I_α form, while those from higher plants such as cotton and ramie are predominantly of the I_β form. As noted earlier, the nomenclature chosen was intended to avoid confusion with the I_A and I_B forms previously used to classify the celluloses on the basis of their infrared spectra in the OH stretching region. In relation to that classification, the NMR spectra suggest that the I_A group has the I_α form as its dominant component, while the I_B group is predominantly of the I_β form.

IV. FURTHER STUDIES OF STRUCTURES IN CELLULOSE

With the wide acceptance of the proposal of the two crystalline forms (I_α and I_β) came the challenge of understanding the differences between them and their relationship to each other within the morphology of native cellulosic tissues. A number of complementary approaches were pursued by different investigators in the search for answers. Some were based on further application of solid-state ^{13}C NMR to the study of different celluloses as well as to celluloses that had been subjected to different modifying treatments. Others were based on application of Raman and infrared spectroscopy to new classes of cellulosic samples. Still, others were based on refinement of electron microscopic and electron diffractometric methods. Results of these investigations will be presented in summary.

A. Raman and Infrared Spectra

The categorization of native celluloses into the I_A and I_B group by Howsmon and Sisson [44] and Blackwell and Marchessault [45] on the basis of the appearance of the OH stretching region of their infrared spectra suggested that the hydrogen bonding patterns within the crystalline domains may be part of the key to the differences between the two forms of native cellulose. This was, in fact, confirmed in the course of more detailed investigations of the Raman spectra carried out on single oriented fibers of native celluloses [49] and in a comprehensive study of the infrared spectra of a number of celluloses of the two forms [50]. The Raman spectral investigations were part of a broader study directed primarily at rationalizing the bands associated with the skeletal vibrational motions and at exploring the differences between celluloses I and II [49]. They differed from earlier Raman spectral studies in that the spectra were recorded with a Raman microprobe on which individual fibers could be mounted for spectral investigation. With this system, it was also possible to explore the variation of the intensity of the bands as the polarization of the exciting laser beam was rotated relative to the axis of the fibers.

The observed spectra are shown in Figs. 9 and 10, each of which includes six spectra. Fig. 9 shows the region between 250 and 1500 cm^{-1}, while Fig. 10 shows the region above 2600 cm^{-1}; the region between 1500 and 2600 cm^{-1} does not contain any spectral features. The spectra in Figs. 9 and 10 are of native and mercerized ramie fibers and of native *V. ventricosa,* and they are recorded with both parallel and perpendicular polarization of the exciting laser beam. Those identified as 0° spectra were recorded with the polarization of the electric vector of the exciting laser beam parallel to the direction of the fiber axes, while those identified as 90° spectra were recorded with the polarization of the electric vector of the laser perpendicular to the fiber axes. The ramie fibers are known to have the molecular chains parallel to the fiber axes; the *V. ventricosa* fibers were prepared by drawing the cell wall so as to align the microfibrils within it.

A number of features in the spectra are noteworthy with respect to earlier discussions. The first is a comparison of the spectra of ***V. ventricosa*** and ramie. It is clear that, apart from a broadening of the bands in the ramie spectra, because of the smaller lateral dimensions of the

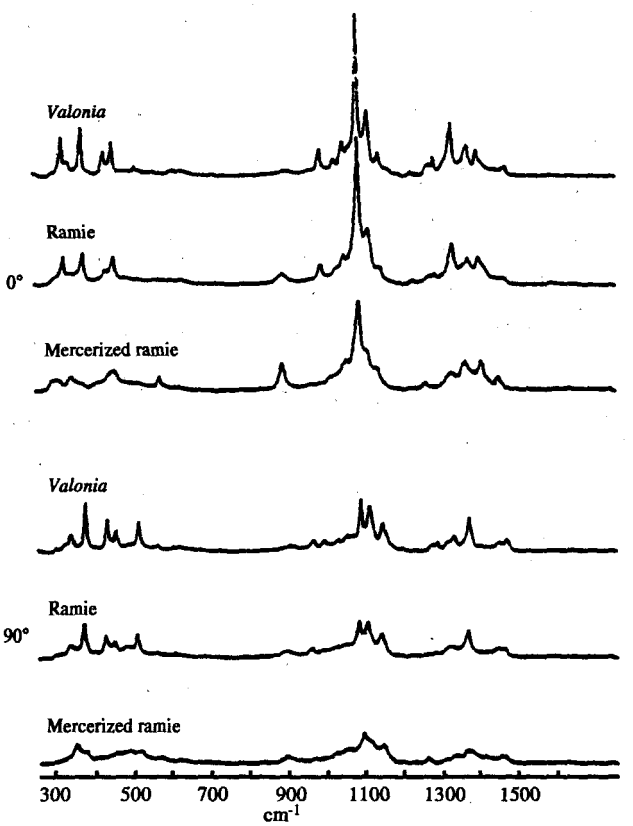

Figure 9 Comparison of the Raman spectra from *Valonia,* ramie, and mercerized ramie (low-frequency region). Spectra were recorded with the electric vector at both 0° and 90°.

crystalline domains, the spectra are very similar except in the OH stretching region. This was interpreted as evidence that the chain conformations in both the I_α and I_β forms are the same, but that the hydrogen bonding patterns between the chains are different within the two forms. This interpretation is more clearly demonstrated in a comparison of the spectra of *V. ventricosa* and *Halocynthia* to be presented below.

The second feature worthy of note is the dramatic difference between the spectra of native (cellulose I) and mercerized (cellulose II) ramie fibers, particularly in the low-frequency region, which is inaccessible to most infrared spectrometers. This was taken as further confirmation that the conformations of cellulose I and cellulose II must differ sufficiently to result in significant alteration of the coupling patterns between the internal vibrational modes of the pyranose rings in the molecular chains. It is also interesting, in this connection, to compare the intensities of the band at 1098 cm^{-1} in the spectra of the two forms of ramie. The band is clearly less intense in the spectrum of the mercerized sample, suggesting that a conformational change, which reduces the coupling of the skeletal motions, has occurred. The 1098-cm^{-1} band is the strongest skeletal band and it is the most intense feature in the spectrum when the polarization of the exciting radiation is parallel to the chain direction. The sensitivity of the Raman spectra to the orientation of an intramolecular vibrational motion is also illustrated in the intensity of the methine CH stretching band at about 2889 cm^{-1}. It is most intense with the electric vector of the exciting radiation at 90° to the chain axis, an orientation that is parallel to that of the methine C–H bonds of the pyranose rings.

Finally, in light of the discussion of the nonequivalence of adjacent anhydroglucose units and the corresponding nonequivalence of alternating glycosidic linkages, the OH region in the 0" spectrum of the mercerized ramie is of particular interest. It shows the two distinct sharp bands that provide evidence of the presence of isolated nonequivalent intramolecular hydrogen bonds in agreement with the alternating glycosidic linkages along the chain; the hydrogen bonds are oriented parallel to the chain direction. This alternation clearly stands out most distinctly in cellulose II. These distinct bands cannot be attributed to nonequivalent chains as the difference in frequency implies a difference in the O–O distances between the oxygen atoms anchoring the hydrogen bond, as well as

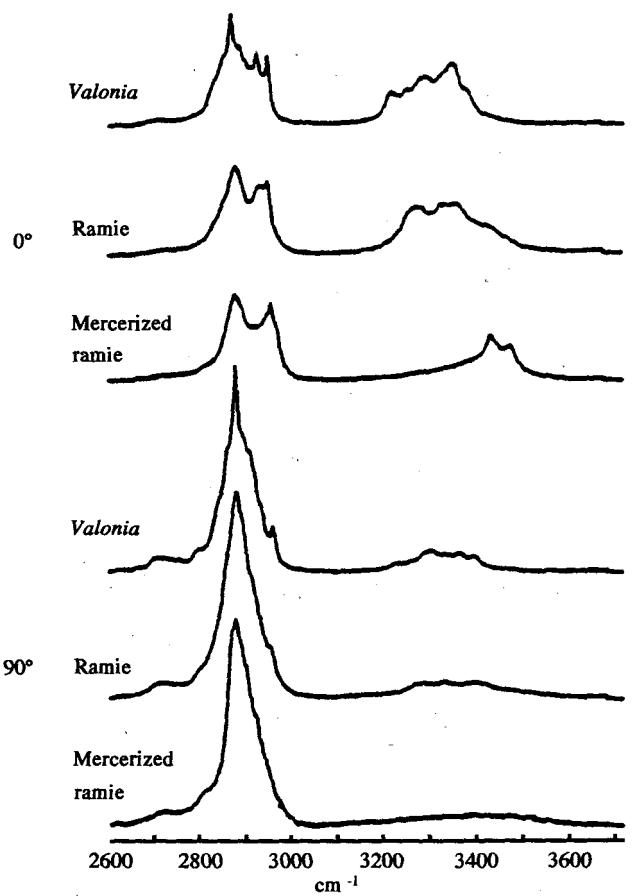

Figure 10 Comparison of the Raman spectra from *Valonia,* ramie, and mercerized ramie (high-frequencyregion). Spectra were recorded with the electric vector at both 0° and 90°.

a difference in the dihedral angles ψ and ϕ of the associated glycosidic linkages. Nonequivalent chains would have different periods in the chain direction if they were to possess twofold helical symmetry.

The infrared spectral studies of the I_α and I_β forms were carried out by Sugiyama et al. [50] on a number of different native celluloses of both forms. Furthermore, it included examination of a number of I,-rich celluloses that were converted to the I_β form through the annealing process first reported by Yamamoto et al. [51]. To complement the infrared spectra, Sugiyama et al. [52] recorded electron diffraction patterns for the samples, which allowed classification of the celluloses through comparison with the diffraction patterns acquired in an earlier electron diffractometeric study to be discussed in greater detail in a subsequent section.

The key finding emerging from the examination of the infrared spectra of the different forms was that the only differences noted were in bands clearly associated with the OH group. This was also true of the changes observed upon conversion of the I_α form to the I_β form through annealing. The bands associated with both the differences in native forms and with the effects of transformation were observed in both the O–H stretching region above 3000 cm^{-1} and the O–H out-of-plane bending region between 650 and 800 cm^{-1}. It was reported that spectra of the I_α form had distinctive bands at 3240 and 750 cm^{-1}, while the spectra of the I, form had distinctive bands at 3270 and 710 cm^{-1}. Furthermore, it was observed that the band at 3240 cm^{-1} appears to be polarized parallel to the direction of the fibril orientation while the band at 3270 cm–1 is not polarized. Among the low-frequency bands. the one at 710 cm^{-1} appears to be polarized perpendicular to the fibril direction, while the one at 750 cm^{-1} is not polarized. It was also observed that upon transformation of the I_α -rich celluloses to the I_β form through annealing, the corresponding bands changed accordingly. The authors concurred with the interpretation of the differences between the two forms suggested by Wiley and Atalla, and concluded that the I_α -to-I_β transformation primarily corresponded to a rearrangement of the hydrogen bond system within the structures and that the two structures appeared to have very similar conformations. The infrared spectral studies by Sugiyama et al. are particularly interesting because they included the spectra of both *Valonia* and *Halocynthia*, the Raman spectra of which have been investigated at high resolution [53].

The Raman spectra of *Valonia macrophysa* and *Halocynthia* (tunicate) celluloses obtained by Atalla et al. [53] are shown in Fig. 11. These particular spectra are of interest because *V. macrophysa* is known to be predominantly the I_α form while *Halocynthia* is predominantly of the I_β form. Comparison of their spectra can be more rigorous than was possible in the earlier work of Wiley and Atalla [49] because the lateral dimensions of the fibrils of both forms are of the order of 20 nm, with the result that their spectra show equal resolution of the bands in all regions of the spectrum. It is to be noted that their spectra are essentially identical in all of the regions associated with skeletal vibrations of all types as well as regions associated with most of the vibrations involving CH bonds, whether in the bending or stretching regions. Indeed, the primary differences between the two spectra are in the broad complex bands occuring in the OH stretching region, and these differences

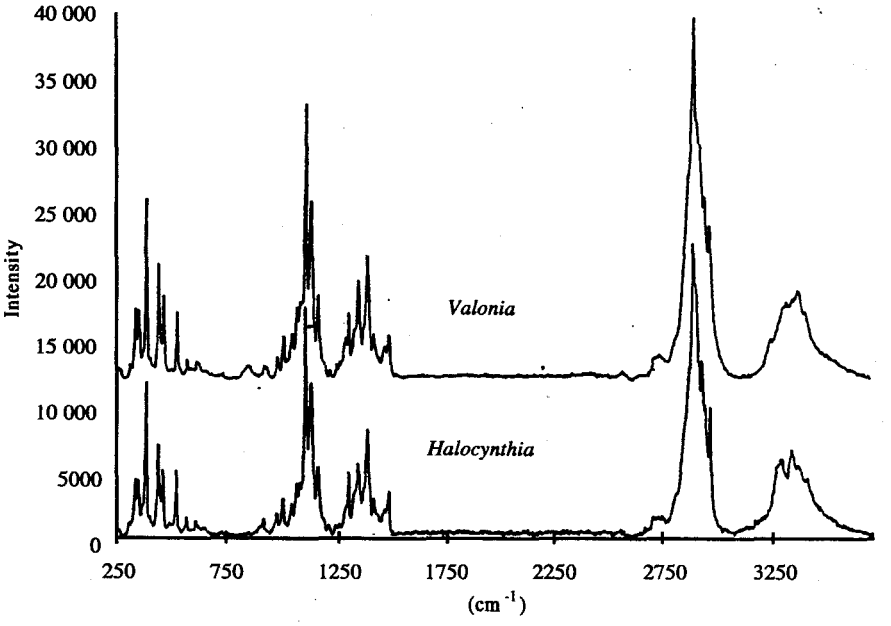

Figure 11 Raman spectra of I_α -rich *Valonia* and I_β -rich *Haleynthia* celluloses. Because both have fibrils of large lateral dimensions, the spectra of both are well resolved and provide a better basis comparison of the spectra of I_α -rich and I_β -rich celluloses.

are not unkike those noted in the earlier Raman spectral studies described above. In addition, the weak band at about 840 cm^{-1} in the spectrum of *V. macrophysa* has no corresponding band in the spectrum of *Halocynthia*; this is the bnd attributed to the out-of-plane bending vibrations of hydrogen-bonded OH groups. There are also minor differences in the relative intensities of the methylene CH stretches and HCH bending vibrations, but these are the natural consequences of different hydrogen bonding patterns for the hydroxyl group at C6. Comparison of the two spectra reinforces the interpretation presented earlier, on the basis of spectra in Figs. 9 and 10, concluding that the only difference between the I_a and I_b forms is in the pattern of hydrogen bonding. Thus, the Raman spectral comparison of the two forms is entirely consistent with that reported for the infrared spectra of these highly crystalline celluloses. It must be kept in mind, of course, that the bands associated with OH grouup vibrations are not expected to coincide in the Raman and infrared spectra; because of the different bases for activity in the two different spectral approaches to measurement of vibrational frequencies, Raman active vibrational modes are frequently silent in the infrared and vice versa. This, of course, is true for the skeletal bands as well.

In view of the considerable variation observed in the Raman spectra of celluloses as a result of changes in molecular conformations, there can be little question that the spectra in Fig. 11 indicate that the conformations of the cellulose molecules in *Valonia* and *Halocynthia* are essentially identical. It is also important to note that the Raman spectra of the celluloses from *V. macrophysa* and V. *ventricosa,* both of which have been used in different studies as representatives of the I_α form, are effectively indistinguishable in all regions of the spectra. This is also true of the Raman spectra of celluloses from the algae *Cladophera glomerata* and *Rhizoclonium heirglyphicum,* which have also been used in many studies as representative of celluloses that are predominantly of the I_α form.

In summary, the Raman and infrared spectral studies undertaken after the discovery of the composite nature of native celluloses point to the conclusion that the only difference between the two forms is in the pattern of hydrogen bonding between chains that possess identical conformations. Yet electron microscopic and electron diffractometric studies, to be described in greater detail in a following section, have led to conclusions that the two forms represent two crystalline phases with different crystal habits [52]. It is therefore important to consider what information may be developed from the vibrational spectra with regard to this question.

The key conclusion drawn from the electron diffractometeric data was that the I_α form represents a triclinic phase with one chain per unit cell, while the I_β form represents a monoclinic phase with two chains per unit cell. Furthermore, the symmetry of the monoclinic phase appeared to be that of space group $P2_1$. It has been recently recognized [53] that such a proposal is not consistent with the vibrational spectra. While it was not possible to have full confidence in this conclusion based on the earlier spectral data because of the differences in the level of resolution between the spectra of ramie and *Valonia* celluloses, the spectra shown in Fig. 11 are of sufficiently high resolution and sufficiently similar that the comparisons can indeed be made with confidence.

The key issue is that when crystal structures possess more than one molecule per unit cell, and the molecules have the same vibrational frequencies, the vibrational modes of the unit cell become degenerate. Under these circumstances, couplings will arise between equivalent modes in the different molecules, and it is generally observed that such couplings result in splittings of the bands associated with key vibrational modes. The type of coupling that is relevant in the case ofcellulose is that described as correlation field splitting [54]. This effect arises because, as a result of the coupling, the vibrations of a particular mode in the two molecules will now occur at two frequencies that are different from those of the isolated molecule; one of the two new frequencies will have the modes in the two different molecules in phase with each other, while the other will have the modes out of phase with each other. Such correlation field effects result in doublets with a splitting of 10–15 cm^{-1} in some modes of crystalline polyethylenes having two chains per unit cell. Because no evidence of such splittings occurs in the *Halocynthia* spectrum shown in Fig. 11, it must be concluded that the I, form cannot have more than one molecule per unit cell. Nor can it be suggested that the two molecules in a monoclinic unit cell are nonequivalent and may have modes that are at different frequencies, because the skeletal bands in the *Halocynthia* spectrum are essentially identical to those in the *Valonia* spectrum. Furthermore, this similarity was also reported in the infrared spectra observed by Sugiyama et al. (cited earlier). Thus, it is clear that the vibrational spectra, both Raman and infrared, point to the conclusion that both the I_α and I_β forms have only one molecule per unit cell. This conclusion of course raises the question as to why the crystallographic data have been viewed for so long as pointing to a two-chain unit cell with the symmetry of space group $P2_1$. This is an issue that is best addressed after the results of the electron diffractometric studies have been described in greater detail.

B. Solid-state ^{13}C NMR Spectra

It is not surprising that the methodology that first provided the basis for understanding the composite nature of native celluloses in terms of the I_α and I_β duality has continued to be the one most often used for seeking deeper understanding of the differences between native celluloses derived from different biological sources. This has been facilitated by the greater availability of solid-state ^{13}C NMR spectrometer systems and by the relative simplicity of the procedures for acquiring the spectra from cellulosic samples. The studies undertaken on the basis of further examination of the solid-state ^{13}C NMR Spectra of celluloses are in a number of categories. The first group is focused on further examination of the spectra of different native celluloses, in part aided by mathematical procedures for

deconvolution of the spectra or for resolution enhancement. Another group relies on exploring the spectral manifestations of native celluloses that have been modified in different ways. Yet, a third approach is based on investigation of celluloses subjected to different but well-known procedures for inducing structural transformations in the solid aggregated state of cellulose.

The group at the Kyoto University Institute for Chemical Research carried out important studies that were complementary to those undertaken by VanderHart and Atalla [42, 43, 45]. More recently, a number of other groups have made contributions. As a number of questions concerning the nature of the I_a and I_b forms remain outstanding, it is useful to begin with an overview of the findings of different groups in this respect. These will then make it possible to view results of studies by using other methods in a clearer perspective.

The early studies by the Kyoto University group have been well summarized in a report that addresses the key points that were the focus of their investigation [55]. In a careful analysis of the chemical shifts of the C1, C4, and C6 carbons in the (CP/MAS) spectra of monosaccharides and disaccharides for which crystallographic structures were available, Horii et al. recognized a correlation between the chemical shifts and the dihedral angles defined by the bonds associated with these particular carbons. In particular, with respect to C6, they demonstrated a correlation between the chemical shift of the C6 resonance and the value of the dihedral angle χ defining the orientation of the OH group at C6 relative to the C4–C5 bond in the pyranose ring. This correlation is of value in the interpretation of the solid-state ^{13}C NMR spectra with respect to structure as well as discussion of the implications of splittings of the C6 resonances observed in some of the spectra.

Of even greater interest, in light of the discussions of deviations from twofold screw axis symmetry in some of the structures, it was observed that the chemical shifts of C1 and C4 are correlated with the dihedral angles about the glycosidic linkage. In particular, there was a correlation between the shift of C1 and the dihedral angle 4 about the C1–O bond, and a correlation between the shift of C4 and the dihedral angle ψ about the O–C4 bond. As the spectra published in the earliest studies did not have sufficient resolution to reveal the splittings of the resonances of C1 and C4, the possibility of occurrence of nonequivalent glycosidic linkages was not addressed at that time.

In addition to the analysis of the correlation between the chemical shifts and the dihedral angles, the Kyoto group investigated the distribution of cellulosic matter between crystalline and noncrystalline domains on the basis of measurements of the relaxation of magnetization associated with the different features of the spectra. By measurement of the values of the spin lattice relaxation times $T_1(C)$ associated with the different spectral features, they developed a quantification of the degree of crystallinity in the different celluloses. They also undertook analysis of the lineshapes of the different resonances, particularly that of the C4 resonance. The lineshape analysis was based on deconvolution of the spectral features into combinations of Lorentzian functions centered at the assigned shifts for the particular resonances. It is to be noted that the use of Lorentzian functions, which can be justified at a fundamental level in the case of spectra from molecules in solution, has no basis in any fundamental understanding of the phenomenology of acquisition of the solid-state ^{13}C NMR spectra. However, .because deconvolution into Lorentzians has been found to be a useful tool in assessing the spectral features in the spectra of cellulose, its use has continued. The qualifications that must be kept in mind when it is used have recently been addressed by VanderHart and Campbell [56].

In the early studies by Horii et al., all of the upfield wing of the C4 resonance was attributed to molecules in noncrystalline domains. On this basis, the lineshape analysis of the C4 resonance of different native celluloses did not seem consistent with the model proposed by VanderHart and Atalla [42] with respect to the composite nature of native celluloses. In later studies, when Horii et al. took note of the fact that, in the study by VanderHart and Atalla, approximately half of the upfield wing of C4 in the spectra of higher plant celluloses was attributed to the surface molecules of crystalline domains, Horii et al. [57] indicated that their results confirm the proposal of VanderHart and Atalla. It is to be noted that in their early reports in this area, Horii et al. used the designations I_b and I, to designate the different groups of celluloses in which the I_α and I_β forms were dominant. However, in their more recent studies, they have adopted the I_α and I_β designations that are designed to avoid the confusion with the categories first introduced by Howsmon and Sisson discussed earlier.

In pursuit of further understanding of the I_α and I_β duality, Horii et al. explored the effects of transformative treatments on the solid-state ^{13}C NMR spectra. The first group of studies was directed at the effects of annealing, first in saturated steam [48], and later in aqueous alkaline solutions (0.1 N NaOH) selected to avoid hydrolytic decomposition of the cellulose [58, 59]. In summary, the key findings were that the celluloses wherein the I_α form is dominant are substantially transformed into the I_β form when conditions are established so as to allow the transformation to be complete. The cellulose representative of the I_α form that was used for these studies was *V. macrophysa.* The effects of the annealing treatment are demonstrated in Fig. 12, which shows the progression in the degree of conversion as the temperature of treatment is increased. Each of the treatments was for 30 min in the aqueous alkaline solution. These results, of course, point to the susceptibility of the I_α form to conversion to the I_β form, suggesting that the latter is the more stable form. To test this hypothesis, a sample of tunicate cellulose, which had earlier been shown to be of the I_β form by Belton et al. [60], was also annealed in an aqueous alkaline solution at 260°C; it showed little change as a result of the annealing [59].

Additional studies by the Kyoto group relied on the solid-state ^{13}C NMR to explore the effects of different variables on the structure of cellulose [61]. It is in order,

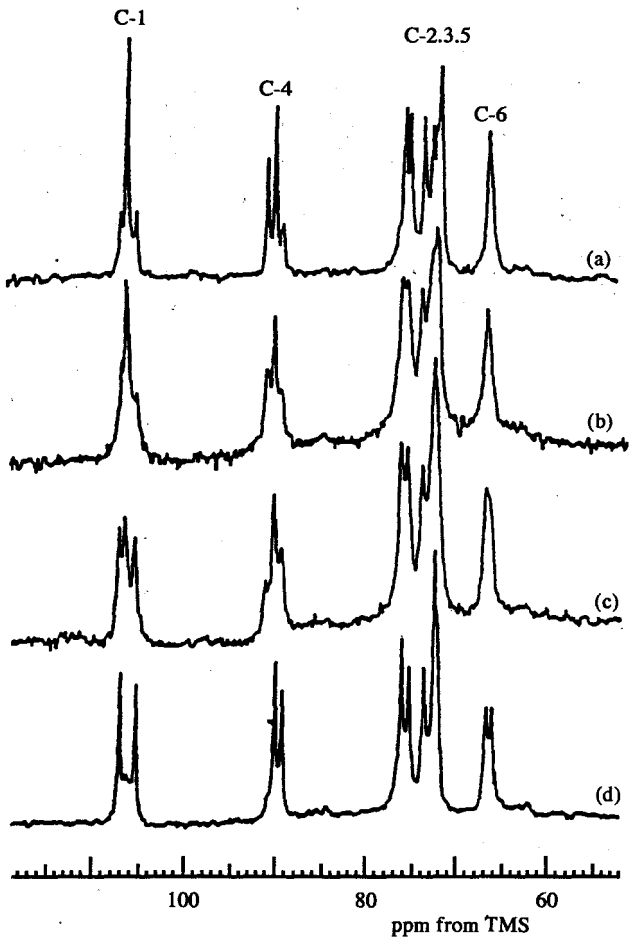

Figure 12 50-MHz CP/MAS ^{13}C NMR spectra of *Valonia* cellulose annealed at different temperatures in 0.1 N NaOH solution: (a) original; (b) 220°C; (c) 240°C; (d) 260°C.

in the present context, to briefly note the results of one study in which celluloses from *A. xylinum* cultures were investigated. One of the variables explored was the temperature of the culture; it was observed that lower temperatures favored the formation of the I_α form at the expense of the I_b form. This finding raises a fundamental question regarding the possibility that the variation of the balance between the two forms is, in part, an adaptive response to changes in the environment.

We follow with a commentary on the manifestations in the solid-state ^{13}C NMR spectra of a broader category of structural changes induced by different treatments known to alter the states of aggregation of cellulose. In selecting the investigations to be noted in our discussion, we will focus on studies that provide insight into the variations of the states of aggregation with the history of particular celluloses, both with respect to source and with respect to processes of isolation and transformation.

In 1990, Newman and Hemingson [62] began to combine some additional methods of processing the ^{13}C NMR spectral data with those that had been used previously such as the monitoring of the value of $T_1(C)$ associated with the different spectral features. While these procedures incorporate a significant degree of empiricism, they have facilitated rationalization of the spectral features of a number of native celluloses and are therefore valuable contributions to the repertoire of methods available for interpreting the ^{13}C NMR spectra of native celluloses. It must be noted, however, that the application of these methods has been complemented in the work of Newman and Hemingson, by a considerable degree of awareness of the complexity of the structures of both native and processed celluloses, so that their application by others needs to be approached with this awareness in mind. This work is described in the publications of Newman et al. [62–67], and has been presented in an overview elsewhere [1].

A different approach to mathematical analysis of the solid state ^{13}C NMR spectra of celluloses was introduced by the group at the Swedish Forest Products Laboratory (STFI) [68]. They took advantage of statistical multivariate data analysis techniques that had been adapted for use with spectroscopic methods. Principal component analysis (PCA) was used to derive a suitable set of subspectra from the CP/MAS spectra of a set of well-characterized cellulosic samples. The relative amounts of the I_α and I_β forms and the crystallinity index for these well-characterized samples were defined in terms of the integrals of specific features in the spectra. These were then used to derive subspectra of the principal components, which in turn were used as the basis for a partial least squares analysis of the experimental spectra. Once the subspectra of the principal components are validated, by relating their features to the known measures of variability, they become the basis for analysis of the spectra of other cellulosic samples that were not included in the initial analysis. Here, again, the interested reader can refer to the original publications [68–71] or the overview presented earlier [1].

C. Electron Microscopic Studies

The use of electron microscopy in the study of celluloses, particularly in their native state, has resulted in important advances beginning with investigations that were undertaken at the time of the introduction of the earliest electron microscopes. The early work has been ably reviewed by a number of authors [72, 73]. Of particular note among these is the coverage of the subject in the treatise by Preston [74].

The earliest and most significant observations, from a structural perspective, were those by Hieta et al. [75], in which they applied a staining method incorporating a chemistry that requires the presence of reducing end groups. They observed that when whole microfibrils of *Valonia* were viewed, only one end of each microfibril was stained. This clearly indicated that the molecular chains were parallel as the reducing ends of the cellulose chains occurred together at one end of the fibrils. Had the structure been one with an antiparallel arrangement of cellulose chains, it would have been expected that the reducing end groups would occur with equal frequency at

both ends of the microfibril with the result that both ends would be equally stained.

The conclusions of Hieta et al. were independently confirmed by another method introduced by Chanzy and Henrissat [76], wherein the microfibrils were subjected to the action of a cellobiohydrolase that is specific in its action on the nonreducing ends of the cellulose chains. They observed a clear narrowing of the tips of the microfibrils to a triangular form at only one end of each microfibril. In this instance, the action was at the nonreducing ends, but the observations were equally convincing evidence that the chains are aligned in a parallel arrangement in these microfibrils.

These early studies were focused on microfibrils from algal celluloses that, because of their larger lateral dimensions, could be more easily visualized in detail. More recently, the technique of specific staining of reducing end groups was adapted for application to cotton microfibrils by Maurer and Fengel [77]. In addition to application of the technique to examination of native cellulose, Maurer and Fengel applied the method to examination of microfibrils of mercerized cellulose (cellulose II), for which they also observed staining at only one end of the microfibrils. This last observation, which indicates a parallel chain structure in cellulose II, is very much in contrast to the crystallographic models that point to an antiparallel structure for this form of cellulose. It reinforces the view that the structure of cellulose II still has many uncertainties associated with it, in spite of the many theoretical analyses that have attempted to rationalize the antiparallel form.

In yet another important set of investigations by Sugiyama et al. [78–80], reported at approximately the same time, it was demonstrated that lattice images could be recorded from the microfibrils of *V. macrophysa*. The first images captured were based on lateral observation of the microfibrils [78, 79]. Later, the techniques were refined to allow the acquisition of lattice images of cross sections of microfibrils [80]. The significance of these observations was that it was now possible to demonstrate conclusively that the microfibrils are uniform in formation, and that there is no evidence that they are composed of smaller subunits aggregating together to form the individual microfibrils that are observed in the electron micrographs. Thus, the observations resolved some of the questions that had arisen earlier concerning the interpretation of electron micrographs of native celluloses [74, 81]; the findings of Sugiyama et al. were the first direct evidence that the approximately 20×20-nm cross sections were not composed of distinguishable smaller subunits. It should be noted, however, that the electron diffraction processes responsible for formation of the lattice images are dominated by the organization of the heavy atoms in the molecular chains and would be insensitive to any nonuniformity in the hydrogen bonding patterns within the interior of the 20 × 20-nm fibrils. The homogeneity of the microfibrils revealed in the lattice images is an issue that needs to be revisited in the context of discussions of biogenesis, for in each instance, the homogeneous crystalline domains clearly include a *much larger* number of cellulose chains than could possibly arise from the individual membrane complexes associated with the biogenesis of cellulose.

Later studies by Sugiyama et al. were based on electron diffraction and were directed at addressing questions concerning the nature of the differences between the I_α and I_β forms of cellulose. In a landmark study [82], electron diffraction patterns were recorded from *V. macrophysa* in both its native state, wherein the I_α and I_β forms occur in their natural relative proportions, and after annealing using the process first reported by Yamamoto et al. [51], which converts the I_α form into the I_β form. The native material, which is predominantly the I_α form, was shown to produce a complex electron diffraction pattern similar to that which had earlier led Honjo and Watanabe [83] to propose an eight-chain unit cell. In sharp contrast, the annealed sample, which is essentially all of the I_β form, produced a more simple and symmetric pattern that could be indexed in terms of a two-chain monoclinic unit cell. The observed patterns are shown in Fig. 13. Figure 13(a) shows the diffraction pattern of the native forms, while Fig. 13(b) shows how the diffraction pattern is transformed upon annealing. It is the latter that is identified with the I_b form and which has been interpreted to indicate a monoclinic unit cell. Figure 13(c) and (d) are schematic representations of the spots in the diffraction diagrams (a) and (b) and show more clearly how the diffraction pattern is transformed by annealing; the spots marked with arrows are the ones that disappear upon annealing. Upon separating the diffraction pattern of the I_β form from the original pattern, it was possible to identify the components of the original pattern that could be attributed to the I_α form, and it was found to correspond to a triclinic unit cell.

In this first report concerning the differences between the diffraction patterns of the I_α and I_β forms, the positioning of the chains within the monoclinic unit cell associated with the I_β form was left open. Two possibilities were regarded as consistent with the diffraction patterns, the first with the twofold screw axes coincident with the molecular chains, the second with the twofold screw axes between the chains. Both possibilities were consistent with the occurrence of nonequivalent anhydroglucose units. The triclinic unit cell associated with the I_α form was also viewed as consistent with two possibilities: the first, a two-chain unit cell and the second, an eight-chain unit cell similar to the one first proposed by Honjo and Watanabe [83].

In a later study by Sugiyama et al. [84], the possibilities were narrowed. It was stated that the monoclinic unit cell corresponding to the I_β form was viewed as one wherein the chains were coincident with the twofold screw axes. It was also indicated that the pattern of the triclinic unit cell corresponding to the I_α form appeared consistent with a unit cell with only one chain per unit cell. In both instances, the rationale for these determinations was not presented.

Another interesting group of observations reported in the second electron diffraction study by Sugiyama et al. [84] were interpreted as evidence of the occurrence of the two forms of cellulose in separate domains within the same

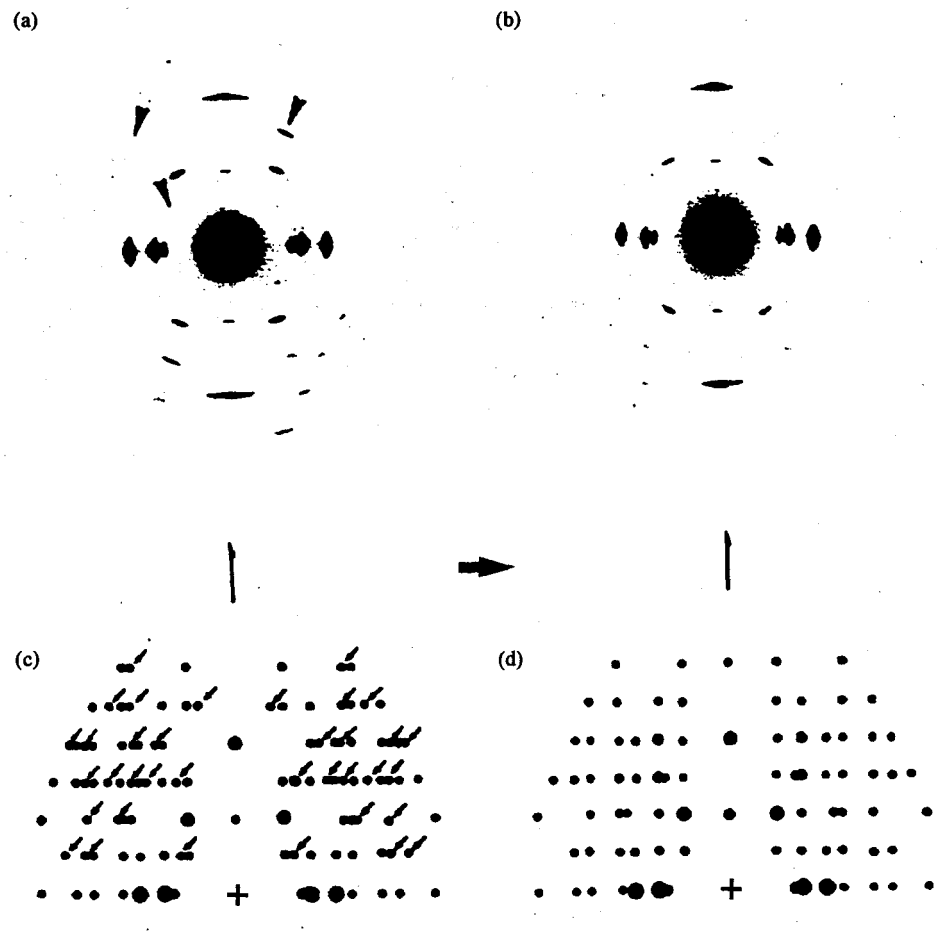

Figure 13 Typical electron diffraction patterns of *V. macrophysa* before (a) and after (b) annealing. In the schematic representations of the patterns, the spots marked with arrows correspond to the reflections that disappear during the annealing treatment (after Sugiyama).

microfibrils. It was reported that the subsets of reflections associated with the two different forms could be separately observed, or in combination along the length of an individual microfibril within domains separated by 50 μm from each other. This set of observations was interpreted to indicate an alternation between the I_α and I_β forms along the length of an individual microfibril. Such an interpretation of course raises questions concerning the processes of biogenesis, particularly because the relative proportions of the two forms of cellulose has been found to be invariant for a particular species as long as the procedures used for isolation of the cellulose do not incorporate exposure to conditions that can result in transformations of the I_α form into the I_β form.

The observation of different domains producing different diffraction patterns along the same microfibril can be envisioned as arising in two ways. The first is the possibility that the microfibril that was used to acquire the diffraction patterns had a limited amount of curvature or twist to it so that the angle between the electron beam and the unit cell axes was not constant. This could result in differences of relative intensities of diffraction spots from different planes and, given the short duration of the exposures, result in an unintended editing of the diffraction patterns. Thus, only those diffraction spots that are intense enough to be observed at a particular angle will be detected, while weaker ones go unseen. For example, if the lattice structure first suggested by Honjo and Watanabe [82] is the true one characteristic of the algal celluloses, diffraction patterns observed at different angles would result in different degrees of enhancement of the different subsets of the total diffraction pattern. This would also be true if the three-dimensional organization of the chains is more appropriately viewed as a superlattice. Indeed, it is possible that the lattice structure first proposed by Honjo and Watanabe represents the unit cell of such a supelattice.

Such an interpretation of these observations is consistent with earlier observations by Roche and Chanzy [85], wherein an electron microscopic image of microfibrils of algal celluloses was formed by use of a technique based on diffraction contrast. It resulted in images of the algal microfibrils that had alternating dark and bright domains that appeared to be of the order of 50 nm in length. This suggests that the Bragg angle associated with a particular

set of reflections is not likely to be coherently ordered relative to the electron beam in domains that are more than 50 nm in length. Given that the coherence of orientation relative to the electron beam was not found to extend beyond 50 nm, it would appear unlikely that it would remain invariant over a distance of 50 μm.

An alternative interpretation of the observation is that the alternation of the I_α and I_β, forms is real, as proposed by Sugiyama et al. [84], and it reflects an assembly process that is not yet sufficiently well understood. It has been suggested that mechanical stress can facilitate the transformation of the I_α form into the I_β form and that the formation of the I_β form may arise from mechanical deformations of the fibrils in the course of deposition; as they emerge from the plasma membrane they are required, in most instances, to be bent to be parallel to the plane of the cell wall. If this is indeed the source of the reported alternation of the I_α and I_β forms along the microfibril, it would raise questions concerning the uniqueness of the balance between the I_α and I_β forms that seems to be characteristic of particular species.

V. COMPUTATIONAL MODELING

The computational modeling has found particular favor in the analyses of large molecules of biological origin. And, of course, cellulose and its oligomers have attracted some attention in this arena. It is valuable to review briefly some of the efforts directed at advancing the understanding of cellulose because, in addition to providing insights regarding the contributions of different classes of interactions, they illustrate the reality that the results of analyses can often be the consequences of assumptions and premises introduced at the outset, rather than conclusions that can provide definitive answers to questions under exploration. As alluded to earlier, the analysis by Rees and Skerret [20] was one of the first computational efforts to explore the constraints on the freedom of variation inherent in the structure of cellobiose. It relied on a potential function that is focused on van der Waals interactions to establish the degree to which domains within ψ/ϕ space may be excluded by hard sphere overlap. The key finding was that approximately 95% of ψ/ϕ space was indeed excluded from accessibility on the basis of hard sphere overlaps that were unacceptable in the sense that they required particular atoms associated with the region of the glycosidic linkage to be significantly closer to each other than the sum of the van der Waals radii. And upon mapping the energy associated with allowable conformations, they found that the two regions indicated by the solid line contours in Fig. 2 represented energy minima close to the conformations defined by the twofold helical constraint. The boundaries of the acceptable region are not very far removed from the domains within the contours; the region between the two domains along the twofold helix line ($n=2$) was not excluded by hard sphere overlap, but it did represent a saddle point in the potential energy surface.

The next group of computational studies did incorporate hydrogen-bonding energies as well the van der Waals interactions. Whether they exhibited the double minima, and the degree to which the double minima were pronounced, depended in large measure on the relative weighting given to the different types of nonbonded interactions. In many, particularly those relying on the potential energy functions incorporated in the linked atom least squares (LALS) programs, the weighting was

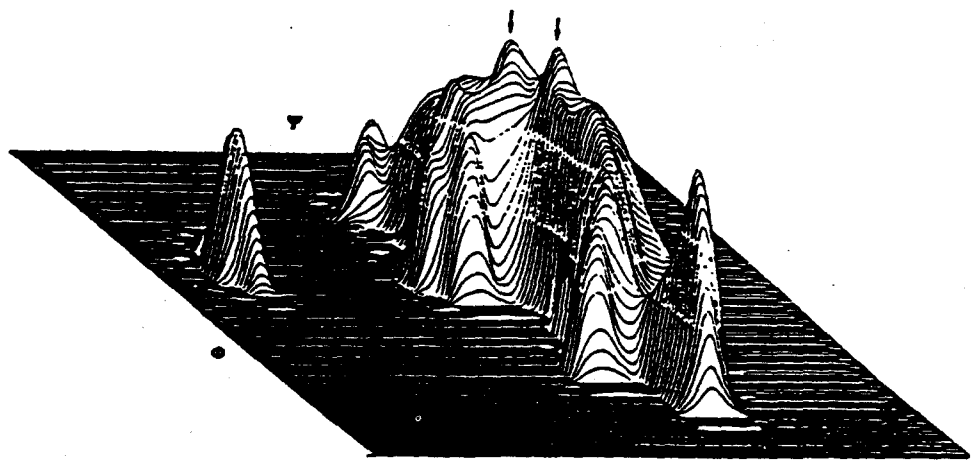

Figure 14 Perspective drawing of the three-dimensional shape of the mirror image of the conformational energy well for the full angular range of Φ and ψ. The volume was constructed using the following scheme: $V(\Phi, \psi)$? 15 kcal^{-1} mol^{-1}; $V_P(\Phi, \psi)$? 1/5 kcal^{-1}; $V_P(\Phi, \psi) = -(V(\Phi, \psi) - 15)$, with V being the energy expressed relative to the minimum. Proceeding from top to bottom of the three-dimensional shape, note the very low energy region (the arrows point towards the conformations observed for crystalline cellobiose and methyl-β-D-cellobioside). The 5–10 kcal^{-1} mol^{-1} energy contours correspond to the light gray region of the volume.

based on fitting the potential functions to optimize the match between computed structures for small molecules for which the crystal structures were known from crystallographic studies. The results were that some showed very shallow minima off the twofold helix line [23]; the twofold helical structures were then rationalized on the basis that the departure represented a small difference in the energies that were regarded as within the error of the computation. When the criterion for quality of fit is chosen as a global minimum of the potential energy, without attention to the fact that it may incorporate unacceptable hard sphere overlaps, the results of the computational analysis can be misleading.

Later studies did not incorporate disproportionate weighting of the different types of nonbonded interactions [28, 29], and the result is perhaps best illustrated in the mapping of the potential energy for cellobiose shown in Fig. 14 taken from the study of cello-oligomers by Henrissat et al. [29]. In this instance, for purposes of visualization, the ψ / ϕ map presents the mirror image of the potential energy surface computed for cellobiose. While well more than two minima are shown in this mapping, it is to be noted that only the two corresponding to the crystal structures of cellobiose and methyl-β-cellobioside, marked by arrows, are within the boundaries established in the analysis by Rees and Skerret described earlier. The other minima correspond to conformations that are more favorable to hydrogen bonding, but with relatively high energies associated with the van der Waals interactions pointing to severe hard sphere overlap.

VI. POLYMORPHY IN CELLULOSE

One of the discoveries growing out of the early diffractometric studies of cellulose was that it can occur in a number of allomorphic forms in the solid state, each producing distinctive X-ray diffractometric patterns [86]. In addition to the cellulose II form, which has been extensively discussed, two other forms are well recognized: cellulose III and cellulose IV. It is of interest to consider them briefly because they reflect the capacity of cellulose to aggregate in a wide variety of secondary and tertiary structures, and because some of the higher plant celluloses produce diffraction patterns that are not unlike those of cellulose IV. Furthermore, they reflect the tendency for some of the celluloses to retain some memory of their earlier states of aggregation in a manner not yet understood.

Cellulose III is of little interest from a biological perspective except to the extent that its behavior may reveal some of the interesting characteristics of the native celluloses from which it can be prepared. It can be prepared from either native cellulose or from cellulose II by treatment with anhydrous liquid ammonia at temperatures near -30°C. It produces distinctive X-ray patterns, Raman spectra, and solid-state ^{13}C NMR spectra. Its most interesting characteristic is that it can be restored to the original form by treatment in boiling water. Because of this characteristic, it is common to designate samples of cellulose III as either III_I or III_{II} to indicate both the source material and the form that will be recovered if the cellulose is boiled in water. In the case of native celluloses, the transformation to the III_I form and back to the I form, also has the unusual effect of converting those which have the I_α form dominant, such as those from algal sources, into forms in which the I_β form is dominant. This effect, first reported by Chanzy et al. [87], is accompanied by the partitioning of the algal microfibrils into smaller ones that are closer in lateral dimensions to those characteristic of higher plants. The solid-state ^{13}C NMR spectra also then appear more like those of the higher plants. No such changes have been reported for native celluloses in which the I_β form is dominant. These behaviors by cellulose III point to a memory effect with respect to the secondary and tertiary structures of cellulose that remains very much a mystery at the present time.

Cellulose IV is most often described as the high-temperature cellulose because it can be prepared by exposing the source cellulose to temperatures in the vicinity of 260°C while it is immersed in glycerol. In this preparation, it is reported to depend in structure on whether it is prepared from cellulose I or cellulose II; hence the frequent designation as IV_I or IV_{II}. When prepared from cellulose I, it is first converted to the III_I form prior to the treatment at high temperature in glycerol. When prepared from cellulose II, it can be directly produced from the II form or via the III_{II} form as an intermediate. However, in the case of cellulose IV, there are no known procedures that allow restoration to the original form; the use of the different designations reflects some differences in the diffraction patterns observed from the two different forms. Furthermore, most of its reported preparations from native forms of cellulose have been from higher plant celluloses wherein the I_β form is dominant and the lateral dimensions of the native microfibrils are quite small; it is not at all clear that treatment of microfibrils of larger lateral dimensions such as those of *Valonia* or those of *Halocynthia* will result in such changes.

In addition to its preparation by heating at 260°C in glycerol, cellulose IV has been recovered when cellulose is regenerated from solution at elevated temperatures. This has been observed with solutions in phosphoric acid regenerated in boiling water or in ethylene glycol or glycerol at temperatures above 100°C [88]. It has also been observed upon regeneration from the dimethylsulfoxide–paraformaldehyde solvent system at the elevated temperatures [88]. In yet another exploration of high temperature effects on the aggregation of cellulose, it was found that when amorphous celluloses are prepared under anhydrous conditions and then induced to crystallize by exposure to water, the exposure at elevated temperatures resulted in the formation of cellulose IV rather than cellulose II, which is the form usually obtained upon crystallization at room temperature[89].

Samples of cellulose IV obtained through regeneration from solution were shown to have Raman spectra that could be represented as linear combinations of the spectra of celluloses I and II, suggesting that it may be a mixed

lattice in which molecules with two different secondary structures coexist. This possibility is consistent with the earlier conclusion that both cellulose I and cellulose II have ribbonlike structures that depart, to a limited degree, from a twofold helix but in different ways. It is not at all implausible that molecules so similar in shape could coexist in the same lattice.

One of the complications in interpreting observations of the occurrence of cellulose IV is that its X-ray diffraction powder pattern is very similar to that of cellulose I. The 020 reflection is nearly identical to that of cellulose I and the 110 and the 1–10 reflections collapse into a single reflection approximately midway between those of cellulose I. As a result, many of the less well-ordered native celluloses produce X-ray patterns that could equally well be interpreted as indicating cellulose I, but with inadequate resolution of the 110 and 1–10 reflections, or as cellulose IV. They are usually characterized as indicating cellulose I because they represent celluloses derived from native sources. Indeed, when cellulose IV was first observed, it was thought to be a less-ordered form of cellulose I.

The close relationship between cellulose IV and the native state is also reflected in reports of its observation in the native state of primary cell wall celluloses. These were observations based on electron diffraction studies of isolated primary cell wall celluloses [90].

VII. CHEMICAL IMPLICATIONS OF STRUCTURE

It was noted earlier that an acceptable fit to the diffractometric data is not the ultimate objective of structural studies. Rather, it is the development of a model that possesses a significant measure of validity and usefulness as the basis for organizing, explaining, and predicting the results of experimental observations. In the sections above, the new and evolving conceptual framework for describing the structures of cellulose was described in relation to spectral observations. It is important also to consider the degree to which the structural information that has been developed above may be useful as the basis for advancing the understanding the response of celluloses to chemical reagents and to enzyme systems. It is useful first to review briefly past works directed at rationalizing the responses to such agents.

The vast majority of studies of the chemistry of cellulose have been directed at the preparation of cellulose derivatives with varying degrees of substitution depending on the desired product. Sometimes the goal is to prepare a cellulose derivative that possesses properties that significantly differ from those of the native form; some derivatives are water-soluble, others are thermoplastic, and others still are used as intermediates in processes for the regeneration of cellulose in the form of films or fibers. At other times, the objective is to introduce relatively small amounts of substitution to modify the properties of the cellulosic substrate without it losing its macroscopic identity or form such as fiber or microcrystalline powder or regenerated filament or film. All such modification processes begin with a heterogeneous reaction system, which may or may not eventually evolve into a homogeneous system as the reaction progresses. Thus, in all chemical investigations that begin with cellulose as one of the ingredients, issues associated with heterogeneous reaction systems arise. Understandably, the one that has been dominant in most investigations is the question of the accessibility of the cellulose.

A variety of methods have been developed to relate accessibility to microstructure. Almost all of them begin with the premise that the cellulose can be regarded as having a crystalline fraction and a disordered or amorphous fraction. It is then assumed that the amorphous or disordered fraction is accessible while the crystalline fraction is not. In some instances, the portion of the crystalline domains that is at their surface is regarded as accessible ‘and it is therefore included as part of the disordered fraction. In other instances, the particular chemistry is thought to occur only in the disordered fraction and the surfaces of crystalline domains are not included. The different approaches have been reviewed by Bertoniere and Zeronian [91], who regard the different approaches as alternative methods for measuring the degree of crystallinity or the crystalline fraction in the particular celluloses.

A number of different chemical and physical approaches are described by Bertoniere and Zeronian. The first is based on acid hydrolysis acids followed by quantification of the weight loss due to dissolution of glucose, cellobiose, and the soluble oligomers [92]. This method is thought to incorporate some error in the quantification of the crystalline domains because the chain cleavage upon hydrolysis can facilitate crystallization of chain molecules that had been kept in disorder as a result of entanglement with other molecules. Another method is based on monitoring the degree of formylation of cellulose when reacted with formic acid to form the ester [93]. In this method, the progress of the reaction with cellulose is compared with a similar reaction with starch, which provides a measure of the possibility of formylation in a homogeneous system wherein the issue of accessibility does not arise.

In another method developed by Rowland and his coworkers [94–97], accessible hydroxyl groups are tagged through reaction of the particular cellulose with *N*,*N*-diethylaziridinium chloride to a produce diethylamineether (DEAE)–cellulose. This is then hydrolyzed, subjected to enzyme action to remove the untagged glucose, silylated, and subjected to chromatographic analysis. This method has the added advantage that it can be used to explore the relative reactivity of the different hydroxyl groups. It is usually observed that the secondary hydroxyl group on C2 is the most reactive and the one at C3, the least reactive, with the primary hydroxyl at C6 having a reactivity approaching that of the group on C2 under some conditions. Here, of course, steric effects are also factors in these substitution reactions.

Among the physical methods discussed by Bertoniere and Zeronian [91] are ones based on sorption and on solvent exclusion. One of the earliest studies relying on the use of sorption as a measure of accessibility was the

classical study by Mann and Marrinan [98], in which deuterium exchange with the protons was monitored. The cellulose was exposed to D_2O vapor for a period sufficient to attain equilibrium and then the degree of exchange was measured by observation of the infrared spectra. Comparison of the band associated with the OD stretching vibration with those associated with the OH stretching vibration provided the measure of the relative amounts of accessible and inaccessible hydroxyl groups. Another approach to monitoring availability to adsorbed molecules is measurement of moisture regain upon conditioning under well-defined conditions as described by Zeronian and coworkers [99].

The method of solvent exclusion has been used to explore issues of accessibility on a somewhat larger scale. An approach pioneered by Stone and Scallan [100] and Stone et al. [101] relied on static measurement using a series of oligomeric sugars and dextrans of increasing size to establish the distribution of pore sizes in different preparations of a variety of native celluloses.

While methods for characterizing celluloses on the basis of their accessibility have been useful, they do not provide a basis for understanding the level of structure at which the response of a particular cellulose is determined. This follows from the rather simple categorization of the substrate cellulose into ordered and disordered fractions corresponding to the fractions thought to be crystalline and those that are not. This classification does not allow discrimination between effects that have their origin at the level of secondary structure and those that arise from the nature of the tertiary structure. Thus, in terms of chemical reactions, this approach does not facilitate separation of steric effects that follow from the conformation of the molecule as it is approached by a reacting species, from effects of accessibility, which is inherently a consequence of the tertiary structure.

The possibility of advancing the understanding of the chemical implications of structure is best illustrated in the context of hydrolytic reactions. Among the patterns that emerge fairly early in any examination of the published literature on acid hydrolysis and on enzymatic degradation of cellulose are the many similarities in the response to the two classes of hydrolytic agents. In both instances, a rapid initial conversion to glucose and cellodextrins is followed by a period of relatively slower conversion, the rate of conversion in the second period depending on the prior history of the cellulosic substrate. In general, the nonnative polymorphic forms are degraded more rapidly during this second phase. In addition, it is found that the most crystalline or highly ordered of the native celluloses are particularly resistant to attack, with the most highly crystalline regions converted much more slowly than any of the other forms of cellulose.

The relationship of the patterns of hydrolytic susceptibility to the range of conformational variation discussed above can be interpreted in terms of contrast between the states of the glycosidic linkage in cellobiose and β-methylcellobioside. The differences between the states that are likely to contribute to the differences in observed reactivity are of two types. The first is differences in the steric environment of the glycosidic linkage, particularly with respect to activity of the C6 group as a steric hindrance to, or as a potential promoter of, proton transfer reactions, depending on its orientation relative to the adjacent glycosidic linkage. The second type of difference is electronic in nature and involves readjustment of the hybridization of the bonding orbitals at the oxygen in the linkage. It is worthwhile to examine the potential contribution of each of these effects.

The steric environment emerges most simply from examination of scale models of the cellodextrins. They reveal that when C6 is positioned in a manner approximating the structure in β-methylcellobioside, the methylene hydrogens are so disposed that they significantlycontribute to the creation of a hydrophobic protective environment for the adjacent glycosidic linkage. If, however, rotation about the C5–C6 bond is allowed, the primary hydroxyl group can come into proximity with the linkage and provide a potential path for more rapid proton transfer.

If, as suggested earlier on the basis of spectral data, the orientation of some C6 groups in native cellulose is locked in by its participation in a bifurcated hydrogen bond to the hydroxyl group on C3, it may contribute to the higher degree of resistance to hydrolytic action. Access to the linkage oxygen would be through a relatively narrow solid angle, barely large enough to permit entry of the hydronium ions that are the primary carriers of protons in acidic media [102]. If, on the other hand, the C6 group has greater freedom to rotate, as is likely to be the case in cellulose II, the hindrance due to the methylene hydrogens can be reduced and, in some orientations, the oxygen of the primary hydroxyl group may provide a tunneling path for transfer of protons from hydronium ions to the glycosidic linkage. This would result in greater susceptibility of nonnative celluloses to hydrolytic attack.

The hypothesis concerning steric effects in acid hydrolysis has as its corollary the proposal that the role of the C_1 component in cellulase enzyme system complexes is to disrupt the engagement of the C6 oxygen in the bifurcated intramolecular hydrogen bond and thus permit rotation of the C6 group into a position more favorable to hydrolytic attack.

The key role of C6 in stabilizing the native cellulose structures is supported by findings concerning the mechanism of action of the dimethylsulfoxide–paraformaldehyde solvent system for cellulose, which is quite effective in solubilizing even the most crystalline of celluloses. The crucial step in the mechanism that has been established for this system is substitution of a methylol group on the primary hydroxyl at the C6 carbon [103, 104].

The effect of conformation on the electronic structure of the linkage is also likely to be a factor with respect to its susceptibility to hydrolytic attack. Although there is no basis for anticipating the directions of this effect at this time, it is well to consider it from a qualitative perspective. First, it is clear that the hybrids of oxygen orbitals involved in the bonds to carbon must be nonequivalent because the bond distances differ to a significant degree [24, 25]. The

angle of approximately 116° imposed on the linkage is likely to result in greater differences between the bonding orbitals and the lone pair orbitals than might be expected in a typical glycosidic linkage that is free from strain. Among themselves, the lone pair orbitals are likely to be different because of their different disposition with respect to the ring oxygen adjacent to C1 in the linkage; the differences may be small and subtle, but they are no less real. Given these many influences on the nature of the hybridization at the oxygen in the linkage, it seems most unlikely that they would remain unaltered by changes in the dihedral angles of the magnitude of the difference between cellobiose and b-methylcellobioside. Hence a difference in electronic character must be expected.

At present, it is not possible to estimate the magnitude of the effects discussed nor to speculate concerning the direction of the change in relative reactivity of the glycosidic linkage in the two different conformations. Yet it is clear that differences can be anticipated and they may be viewed, within limits of course, as altering the chemical identity of the glycosidic linkage as its conformation changes. It remains for future studies to define the differences more precisely.

The points raised with regard to the influence of conformation on factors that determine the pathways for chemical reaction have not been specific subjects of investigation because methods for characterizing secondary structure as apart from the tertiary structure have not been available. It has also been true that suitable conceptual frameworks have not been available for developing the questions beyond the levels of the order–disorder duality. With the development of the approaches outlined above for exploring and distinguishing between matters of secondary structure and those of tertiary structure it is quite likely that in the years ahead, it will be possible to achieve a higher level of organization of information concerning the chemistry of cellulose.

With respect to questions of tertiary structure, the key issue introduced by the new structural information, and one that has not been explored at all at this time, is whether the different hydrogen bonding patterns associated with the I_α/I_β duality have associated with the differences between the reactivity of the hydroxyl groups involved. It is not clear at this time how experiments exploring such effects might be carried out so as to separate issues associated with the differences between the hydrogen bonding patterns from issues associated with differences in accessibility.

VIII. CELLULOSE STRUCTURES IN SUMMARY

From crystallographic studies, based on both X-ray and electron diffraction measurements, it can be concluded that the secondary structures of native celluloses are ribbonlike conformations approximating twofold helical structures. Their organization into crystallographic unit cells remains uncertain, however. The monoclinic space group $P2_1$, with two chains per unit cell, has been proposed for both the earlier studies prior to the discovery of the I_α/I_β duality in native forms, and more recently for the I_β form. The I_α form is thought to possess a triclinic unit cell structure. Some important questions remain regarding the degree to which these are adequate representations of the organization of the crystalline domains in native celluloses. The majority of crystallographic studies also point to parallel alignment of the cellulose chains in the native celluloses, and this conclusion has been confirmed by electron micrographic observations. Also, for cellulose II, the structures derived from the X-ray diffraction data suggest a ribbonlike secondary structure approximating twofold helical organization and, in this instance, antiparallel alignment of the chains, although the antiparallel proposal has been contradicted by recent electron micrographic observations. The unit cell organization of space group $P2_1$, with two chains per unit cell, has also been suggested for cellulose II, although the degree of confidence is even less than that with respect to the structures of cellulose I.

The early Raman spectroscopic studies clearly could not be reconciled with the premise that both cellulose I and cellulose II possess twofold helical conformations as the crystallographic studies had suggested. The Raman spectra, together with some corresponding infrared spectra, also pointed to the probability that the repeat unit of the structure of crystalline celluloses is anhydrocellobiose, so that alternating nonequivalent glycosidic linkages occur within each chain. To preserve the ribbonlike structural approximation, the different conformations of celluloses I and II were rationalized as alternate left- and right-handed departures from the twofold helical structure, with those in cellulose II representing somewhat larger departures from the twofold helical conformation than those in cellulose I.

The introduction of high-resolution solid-state ^{13}C NMR spectral analyses into the study of celluloses resulted in the resolution of one of the fundamental mysteries in the variability of native celluloses by establishing that all native celluloses are composites of two forms. These were identified as the I_α and I_β forms to distinguish them from the I_A and I_B categories that had been introduced more than three decades earlier to classify the celluloses produced by algae and bacteria from those produced by higher plants. The correspondence between the two classifications is that those in the I_A category have the I_α from as the dominant component, while those in the I_B category are predominantly of the I_β form. The nature of the difference between the I_α and I_β forms remains the subject of serious inquiry. Recognition of the I_α/I_β duality has facilitated a significant amount of additional research seeking to establish the balance between the two forms in a wide range of higher plant celluloses.

In later studies, the Raman spectra and corresponding infrared spectra indicated that the primary differences between the I_α and I_β forms of native cellulose were in the pattern of hydrogen bonding. Furthermore, the Raman spectra of the two forms raise questions as to whether the structures can possess more than one molecule per unit cell because there is no evidence of any correlation field splittings of any of the bands in the spectra of the two forms.

Electron microscopic studies relying on agents that act selectively either at the reducing or at the nonreducing end groups of the cellulose chains have provided convincing evidence that cellulose chains are aligned parallel to one another in native cellulose. More recently, similar evidence has been presented supporting the view that the alignment of the chains is also parallel in cellulose 11. Other electron microscopic studies using the methods of lattice imaging have been used to demonstrate that the highly ordered microfibrils derived from algal celluloses represent homogeneous lattice structures with respect to the diffraction planes defined by the organization of their heavy atoms.

Electron diffraction studies carried out on algal celluloses after the discovery of the I_α / I_β duality have been interpreted to indicate that the two forms may alternate along the length of individual microfibrils. These observations can also be interpreted as manifestations of the slow twisting about the long axis that has been observed in other studies of similar algal celluloses.

The possibility of the coexistence of the I_α and I_β forms within a superlattice structure has been suggested in the context of studies intended to mimic the conditions of biogenesis. These will be examined in greater detail in relation to the discussions of native celluloses and of their biogenesis.

Our discussion of structure has focused so far on issues of structure at the nanoscale level, identified as corresponding to domains that are of the order of 2 nm in dimension. Organization at the microscale level, defined as the range between 2 and 50 nm, requires consideration of a number of issues that have not been adequately dealt with in the literature on structures of cellulose. These include the well-recognized departures from a linear lattice, which have been generally regarded as measures of disorder when, in fact, they are more appropriately regarded as indicators of the nonlinear organization in a biological structure. Another issue arising at the microscale is associated with the occurrence of significant fractions of the cellulose molecules at the surface of the microfibrils of most native celluloses, particularly in the case of higher plants. It is the question as to whether the microfibrillar structure can be viewed as a separate phase in the traditional sense and whether criteria developed for the stability of homogeneous phases in the context of classical thermodynamics can have meaning when applied to native cellulosic structures. These issues arise in relation to discussions of native celluloses and their biogenesis.

Part B

Chemical Characterization

1. INTRODUCTION

Cellulosic materials have been used in various fields from commodities to industrial materials after mechanical and chemical modifications. Fig. 15 illustrates the chemical structure of cellulose in terms of chemical modifications [105]. The β-1,4-glycoside bonds and other functional groups such as carboxyls and aldehydes present in most cellulosic material as minor groups are also possible sites for chemical modifications.

II. SOLVENTS

Table 1 summarizes the representative solvents or solvent systems of cellulose. The xanthate system has been used for

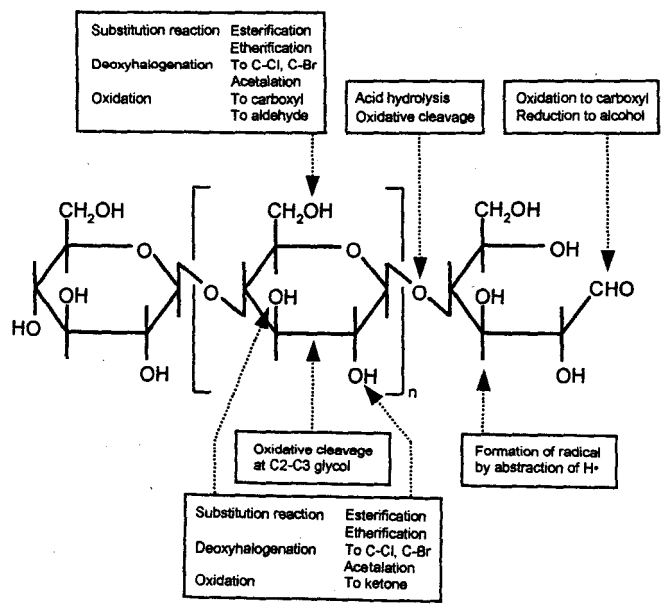

Figure 15 Positions in cellulose structure for chemical reactions.

Table 1 Conventional and New Cellulose Solvent Systems

Category	Solvent	Remarks
Acid	>52% H_2SO_4	Partial hydrolysis
	>85% H_3PO_4	Partial hydrolysis
Alkali	6% LiOH	Needs pretreatments of cellulose
	6–9% NaOH	Needs pretreatments of cellulose
Alkaline metal system complex	$Cu(NH_3)_4(OH)_2$ [cuoxam]	Cuprammonium rayon production
	$Cu(H_2NCH_2CH_2NH_2)_2(OH)_2$[cuen]	Standard solvent for DPv measurement
	$Co(H_2NCH_2CH_2NH_2)_2(OH)_2$	
	$Ni(NH_3)_6(OH)_2$	
	$Cd(H_2NCH_2CH_2NH_2)_3(OH)_2$ [cadoxen]	Transparent solution
	$Zn(H_2NCH_2CH_2NH_2)_3(OH)_2$	
	Fe/3(tartaric acid)/3NaOH [EWNN]	Relatively stable
Alkaline xanthogenate derivatives	CS_2/NaOH	Dissolves cellulose, forming Viscose rayon production system
Inorganic salt	>64% $ZnCl_2$	Dissolves cellulose by heating at 100°C
	>50% $Ca(SCN)_2$	Dissolves cellulose by heating at 100°C
Organic solvent systems	Cl_3CHO/DMF	Dissolves cellulose, forming chloral hemiacetals at all cellulose–OH
	$(CH_2O)_x$/DMSO	Dissolves cellulose, forming (poly)-methylol hemiacetals at cellulose–OH
	N_2O_4/DMF, N_2O_4/DMSO	Dissolves cellulose, forming nitrite ester at all cellulose–OH
	LiCl/DMAc, LiCl/DMI	Stable; needs pretreatments of cellulose
	SO_2/amine/DMSO	Unstable; gives stable amorphous regenerated cellulose
	CH_3NH_2/DMSO	Dissolves cellulose, forming complex
	CF_3COOH (trifluoroacetic acid: TFA)	Dissolves cellulose, forming TFA ester at C6–OH; volatile solvent
	$(Bu)_4N^+ F^-?3H_2O$/DMSO	Dissolves cellulose with DP < 650
	ca. 80% *N*-methylmorpholine-*N*-oxide/H_2O	Uses for lyocell production
		Dissolves cellulose by heating at 90°C
Others	NH_4SCN/NH_3/water	Forms mesophase states
	N_2H_4	Explosive

DMF: *N*,*N*-dimethylformamide, DMAc: *N*,*N*-dimethylacetamide, DMI: *N*,*N*-dimethylimidazolidinone, DMSO: dimethylsulfoxide, Bu: butyl–.

a long time to make viscose rayon and sponge. However, the rayon production, where H_2S is emitted more or less during the recovery system of spent liquor, is shrinking because of environmental issues. On the other hand, cellulose is soluble in aqueous NaOH alone under limited conditions. Microcrystalline cellulose with DP 200–300 is soluble in 6-9% NaOH by freezing and defrosting procedures [106]. Pretreatments of cellulose such as steam explosion are necessary for complete dissolution in the aqueous NaOH for normal bleached wood pulp and cotton linters with DP of more than 500 [107].

Many nonaqueous cellulose solvent systems have been developed in the last three decades. Solvent systems consist of reagent(s) reactive to cellulose hydroxyl groups and a polar aprotic solvent such as dimethylsulfoxide (DMSO) or *N*,*N*-dimethylacetamide (DMAc). Trifluoroacetic acid is the only volatile solvent to dissolve cellulose [108]. Cellulose hydroxyls form unstable derivatives or complexes with the solvent components in the solution states (Fig. 16). These nonaqueous cellulose solvents were used to prepare cellulose derivatives under homogeneous conditions mainly to control degree of substitutions (DS) and distribution of substituents. The LiCl/DMAc system dissolves cellulose by one of the following two procedures: (1) solvent exchange of cellulose soaked in water to DMAc through ethanol, followed by stirring in 8% LiCl/DMAc at room temperature, (2) heating of cellulose/DMAc suspension at ca. 165°C for 30 min, and LiCl is added to the cellulose suspension at about 100°C in the course of cooling to adjust to 8% LiCl/DMAc [109]. Because cellulose solutions in LiCl/DMAc are fairly stable and powderlike LiCl is easy to handle, these solvent systems were extensively studied as reaction media for homogeneous derivatizations of cellulose. Furthermore, the LiCl/DMAc

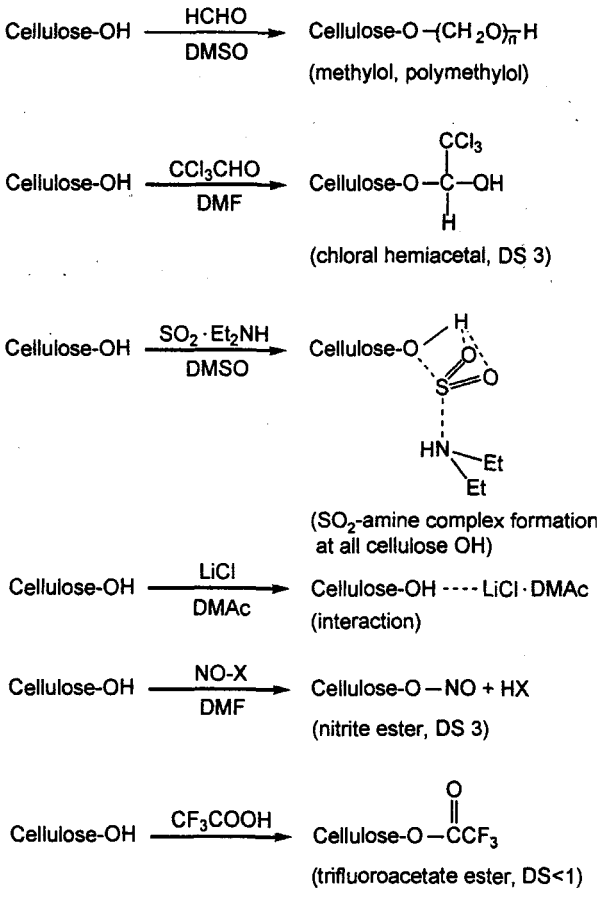

Figure 16 Dissolving states of cellulose in nonaqueous cellulose solvents.

solvent system has been used as an eluent in size-exclusion chromatographic analyses using a multiangle laser-light scattering (SEC-MALLS) detector for molecular mass and molecular mass distribution of cellulose samples [110].

N-Methylmorpholine-*N*-oxide (NMMO), containing ca. 20% water, can dissolve cellulose by melting of NMMO at about 90°C, and has recently been used to make regenerated cellulose fiber (lyocell) at industrial level. NMMO is a kind of oxidant, and thus some antioxidant must be added to the solution before spinning in order to avoid strong coloration and oxidative degradation. It is possible to insert an air-gap stage in between spinning nozzles and the water bath for regeneration—hence this system is called "dry–wet spinning process." Drawing can be achieved in the air-gap stage, resulting in a higher degree of crystallinity as well as a higher degree of orientation of crystals in the regenerated cellulose fiber thereby prepared (Table 2) [111].

III. DERIVATIZATION

Because cellulose has three different hydroxyl groups at C2, C3, and C6 in the anhydroglucose unit (Fig. l), various chemical reactions can possibly apply. Factors influencing the characteristics of cellulose derivatives are as follows: (1) chemical structures of substituents introduced, (2) degree of substitution (DS: the amount of substituents per anhydroglucose unit), (3) distribution of substituents, (4) degree of polymerization and its distribution, (5) purities including the presence of chromophores, and others.

A. Esterification

Typical cellulose esters examined so far are depicted in Fig. 17. Cellulose triacetate (DS > 2.9) is prepared by heating cellulose suspended in a mixture of acetic anhydride/acetic acid/H_2SO_4 around 60°C. Cellulose triacetate is soluble in chlorinated hydrocarbons such as dichloromethane. Cast films of cellulose triacetate have optically characteristic properties of no polarization of penetrated light, and thus have been used as film bases for photograph and supporting films for liquid crystal display. Cellulose diacetate (DS 2.3–2.5) is consecutively prepared from the cellulose triacetate solution by diluting with water and heating. Cellulose diacetate films have been used for ultrafiltration to purify tap water partly in place of chlorination. When pulps having lower a-cellulose content are used, some acetone-insoluble gel fractions originating from hemicellulose are formed from both softwood and hardwood bleached kraft pulps [112]. Thus, bleached sulfite pulp or at least bleached prehydrolyzed kraft pulp prepared from softwood is acceptable as the pulp resources at this point. Therefore, the possibility of using normal

Table 2 Crystallinity Index and Degree of Orientation of Crystals of Regenerated Cellulose Fibers Calculated from their X-ray Diffraction Patterns

Cellulose solvent	Crystal structure	Crystallinity index (%)	Degree of orientation of crystals (%)
$NaOH/CS_2$/water (viscose rayon)	Cellulose II	24	85
Aqueous $Cu(NH_3)_4(OH)_2$ (cuprammonium rayon)	Cellulose II	41	90
69% aqueous NaOH	Cellulose II	46	75
80% NMMO/water (lyocell)	Cellulose II	46	91

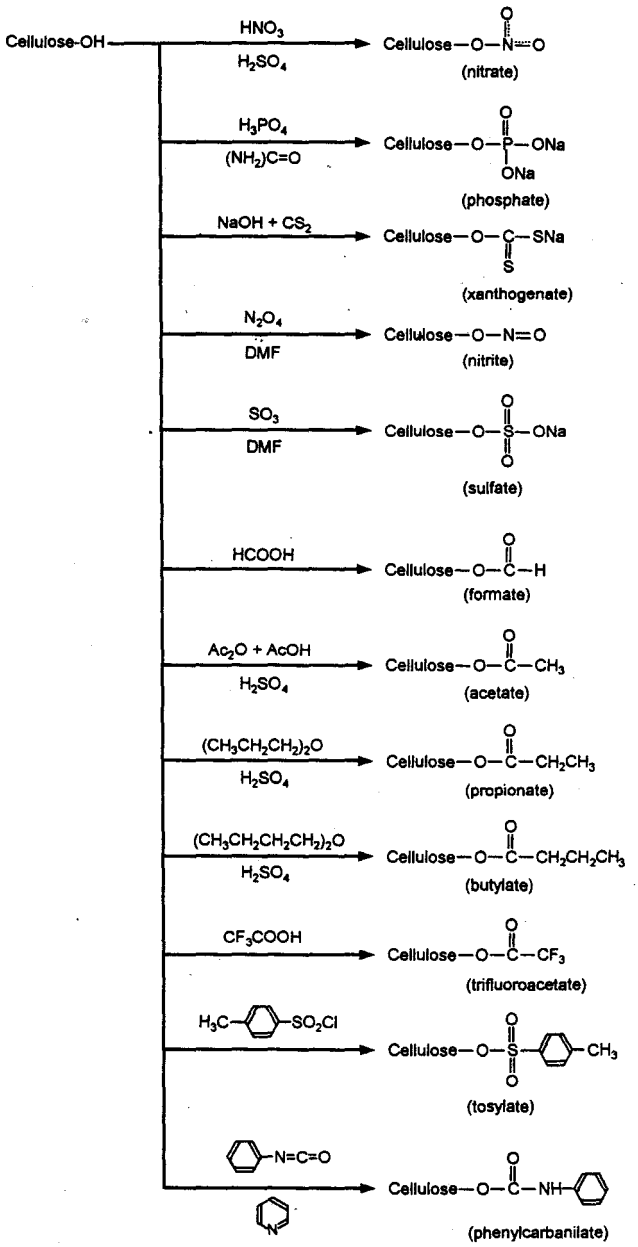

Figure 17 Typical cellulose esters.

bleached kraft pulp produced from eucalyptus without any spinning problems is one of the significant themes for cellulose diacetate production. Furthermore, one-step production of cellulose diacetate without going through the cellulose triacetate stage is also required.

Various cellulose esters such as acetate, tosylate (*p*-toluenesulfonate), sinnamoylate, and fluorine-containing substituents were prepared with pyridine as a base under homogeneous and nonaqueous conditions using, for example, 8% LiCl/DMAc. Although interesting results were obtained at the laboratory level, none of these nonaqueous cellulose solvent systems has been applied to the derivatization media at industrial level. The multicomponent solvent systems, the high boiling point of the solvent such as DMAc and DMSO, the necessity of pretreatments including complete drying of cellulose, and the solvent-exchanging processes for dissolution are the challenges that would render practical applications of the nonaqueous solvent systems to derivatizations a difficult prospect.

B. Etherification

Fig. 18 illustrates representative cellulose ethers. In most cases in industries, cellulose ethers are produced via alkalicellulose (cellulose swollen with, e.g., 18% aqueous NaOH) by reacting with etherifying reagents around 60°C in the presence of *i*-propanol or *i*-butanol, where etherifications proceed heterogeneously to the swollen alkalicellulose without dissolution.

Carboxymethylcellulose sodium salt (CMC), methylcellulose (MC), hydroxyethylcellulose (HEC), and hydroxypropylcellulose (HPC) are typical water-soluble cellulose ethers manufactured at the industrial level, and primarily used as thickeners in various fields. Commercial CMC has DS values in the range of 0.6–1.2. HEC and HPC are produced from alkalicellulose by reacting with ethylene oxide and propylene oxide, respectively. In the case of these cellulose ethers, additional substitution also occurs in hydroxyl groups of the introduced substituents, such as grafting, with increasing the amount of substituents, and thus molecular substitution (MS) in place of DS is used for these cellulose ethers. Water-soluble cellulose ethers in solution states have been characterized by SEC-MALLS, and the presence of coagulation among cellulose ether molecules in water under particular conditions has been reported [113]. When a small amount of long alkyl chains (C_{12}–C_{24}) are introduced into HEC, viscosity of the aqueous solution extremely increases by the formation of hydrophobic interactions among HEC molecules in water [114].

Nonaqueous media offer an advantageous method to prepare cellulose ethers with high DS, which generally cannot be achieved by the conventional aqueous alkalicellulose system. About 30 kinds of cellulose ethers with DS 3 were prepared by one-step reactions with powdered NaOH and etherifying reagents using the cellulose solution in SO_2/diethylamine/DMSO [115]. The triphenylmethyl (trytyl) group can be selectively introduced at C6 primary hydroxyl of cellulose by homogeneous reaction with pyridine in 8% LiCl/DMAc. This tritylcellulose was used as an intermediate for further conversion to some regioselective cellulose ethers and esters such as 2,3-di-*O*-methylcellulose and 6-*O*-methylcellulose (Fig. 19) [116].

IV. OXIDATION

There are several methods to modify the chemical structure of cellulose by oxidation. Periodate oxidation of cellulose suspended in water and N_2O_4 oxidation of cellulose suspended in chloroform are well-known conventional meth-

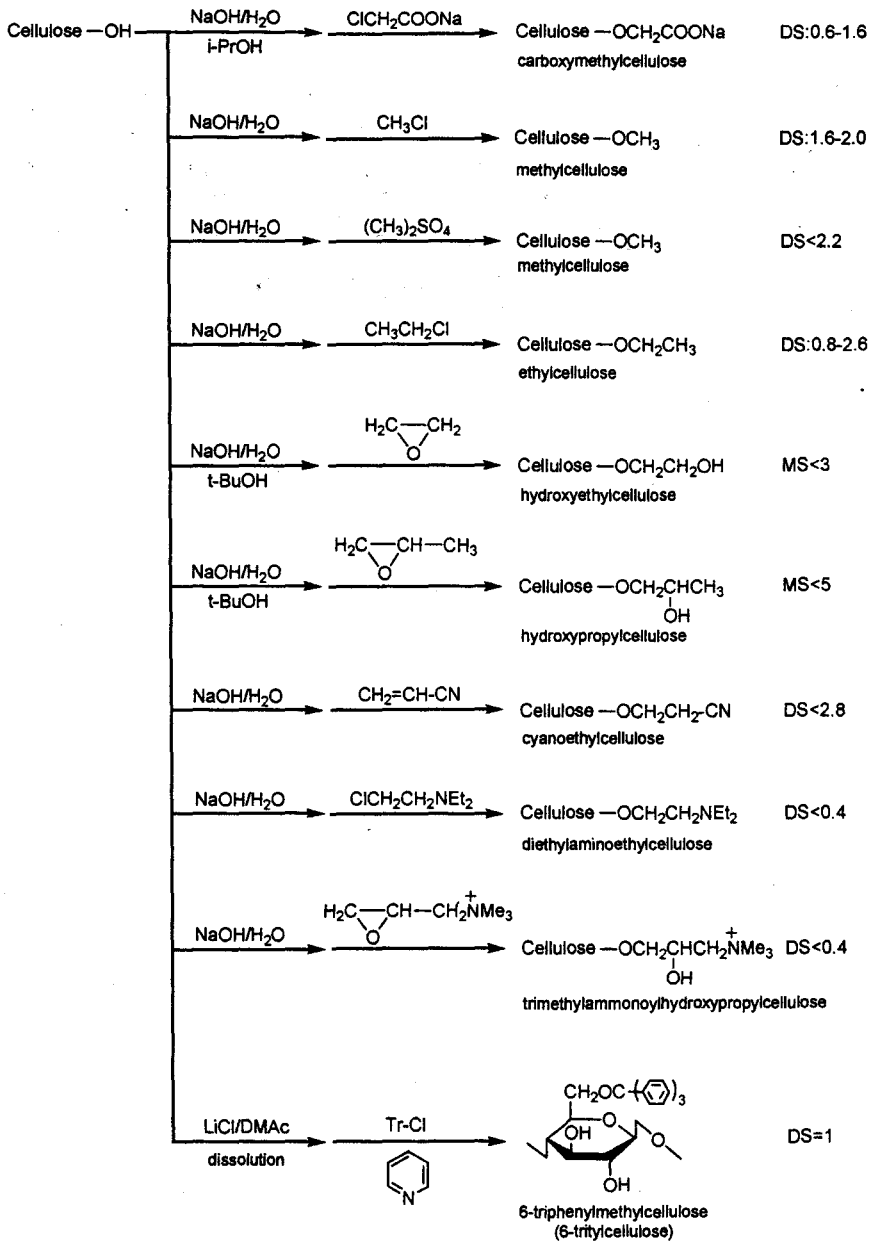

ods to convert cellulose to dialdehyde cellulose and C6-carboxy cellulose, respectively. Generally, however, some side reactions including depolymerization are inevitable during the oxidation process, which makes it difficult to achieve regioselective oxidation completely.

2,2,6,6-Tetramethylpiperidine-1-oxy radical (TEMPO) is a water-soluble and commercially available radical reagent. When sodium hypochlorite is used as a co-oxidant in the presence of catalytic amounts of NaBr and TEMPO in water, C6 primary hydroxyl groups of polysaccharides dissolved in water at pH 10–11 can be selectively converted to carboxyl groups [117]. When this TEMPO-mediated oxidation is applied to native celluloses, only small amounts of carboxyl groups are introduced into the fibrous celluloses. When regenerated or mercerized, cellulose suspended in water is used as the starting material; on the other hand, water-soluble products are obtained quantitatively at room temperature within 1 h (mostly within 20 min). NMR analyses revealed that these water-soluble oxidized products have homogeneous chemical structures, β-1,4-linked polyglucuronic acid (Fig. 20) [118]. Thus, selective oxidation at C6 primary hydroxyl groups of cellulose can be achieved by TEMPO-mediated oxidation in aqueous media when regenerated or mercerized cellulose

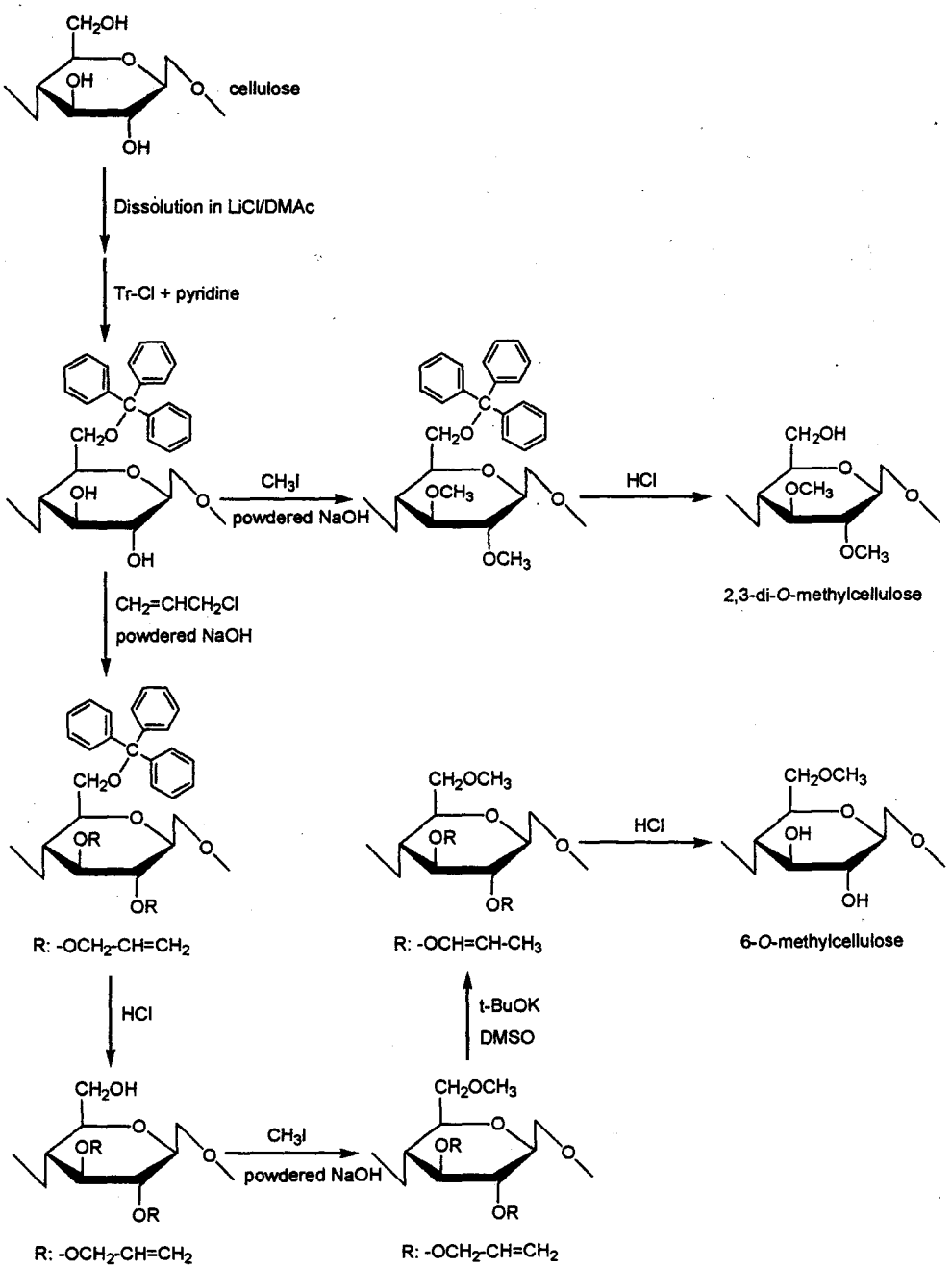

Figure 19 Preparation scheme of regioselectively substituted methylcelluloses via tritylcellulose.

is used (Fig. 21). However, some depolymerization of main chains are inevitable. This new water-soluble polyglucuronic acid is degradable to glucuronic acid and hexenuronic acid residues by commercial crude cellulase [119].

V. DEGRADATION

Cellulosic materials undergo numerous and sometimes harsh stimuli during manufacturing processes and, under specific circumstances, during use. The quality of cellulosic materials is reduced through degradation by means of these outside stimuli. On the other hand, if these degradations can be well controlled, useful cellulose-related compounds can be obtained.

A. Acid Hydrolysis

Acid hydrolysis of cellulosic biomass can be used to produce glucose, which is then converted to ethanol by

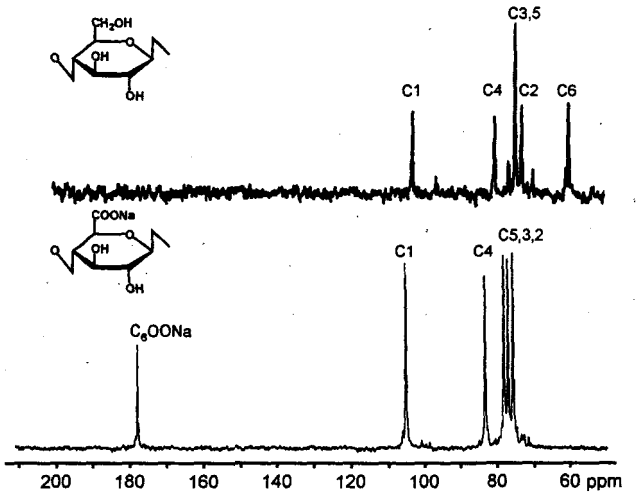

Figure 20 ^{13}C NMR spectra of cellulose oligomer (DP 7) in DMSO and cellouronic acid Na salt (β-1,4-linked polyglucuronic acid) in D_2O. Cellouronic acid Na salt was prepared from viscose rayon by the TEMPO-mediated oxidation.

fermentation. Susceptibility of cellulosic materials to acid hydrolysis is remarkably different between their ordered and disordered regions. When native cellulosic materials such as cotton linters and bleached chemical wood pulps are heated in a dilute acid, hydrolysis of disordered regions in cellulose microfibrils precedes that of ordered regions to form the so-called "microcrystalline cellulose'' with DP 200–300. A part of glucose once formed from cellulose by acid hydrolysis is further degraded to hydroxymethylfurfural, levulinic acid, formic acid, and others during acid hydrolysis (Fig. 22).

B. Enzymatic Degradation

Cellulase hydrolyzes cellulose under mild conditions compared with inorganic or organic acid. Generally, cellulases such as cellobiohydrolase II (CBH II) consist of core and cellulose-binding domains and a linker, which binds the two domains. The core domain contains an active center to hydrolyze cellulose in catalytic manner and the subsites, which interact with cellulose chain close to the active center. The cellulose-binding domains consist of amino

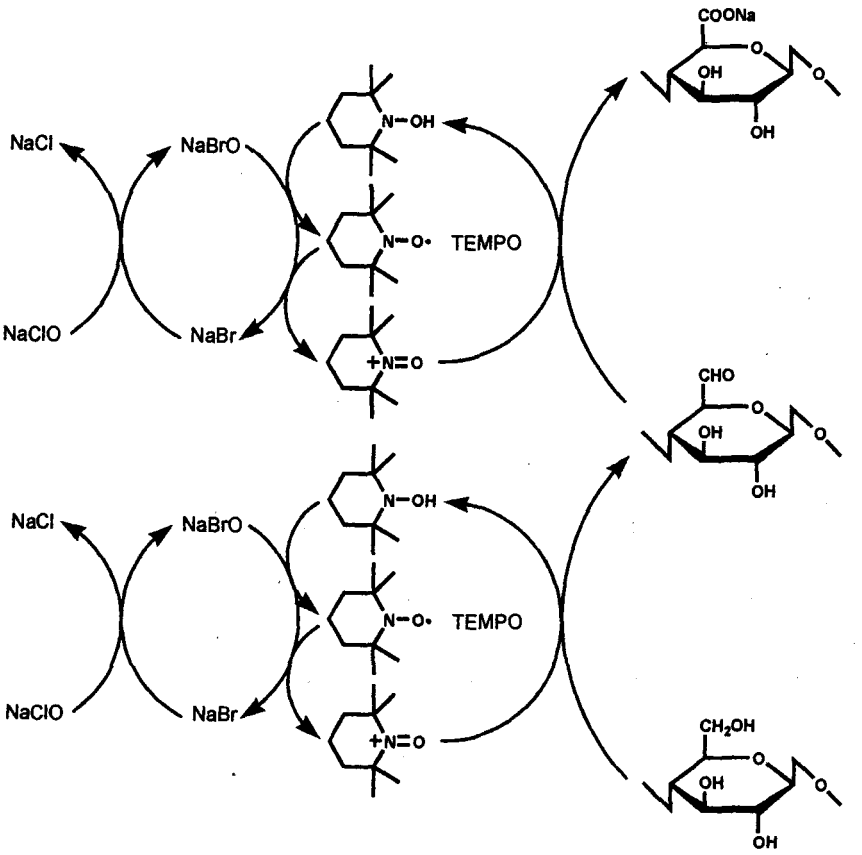

Figure 21 TEMPO-mediated oxidation of C6 primary hydroxyl group of cellulose to carboxyl group.

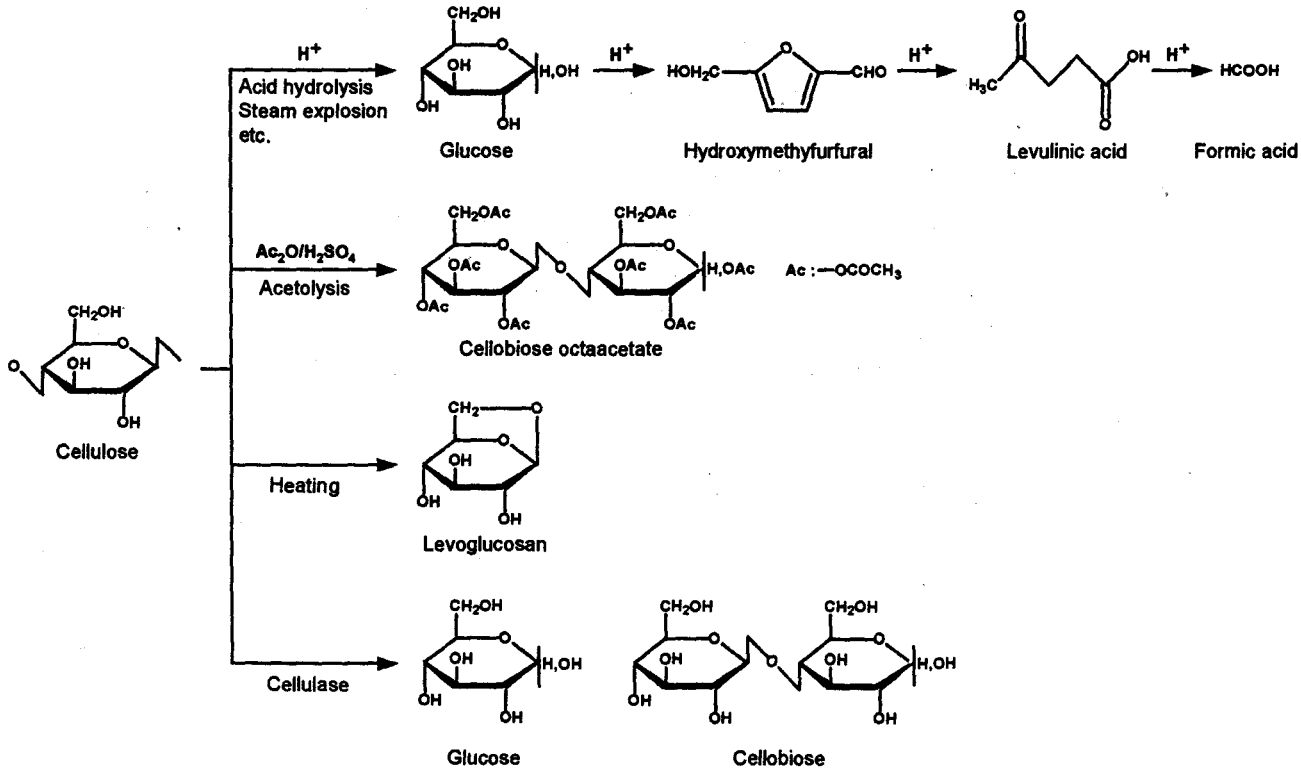

Figure 22 Some degradation products of cellulose.

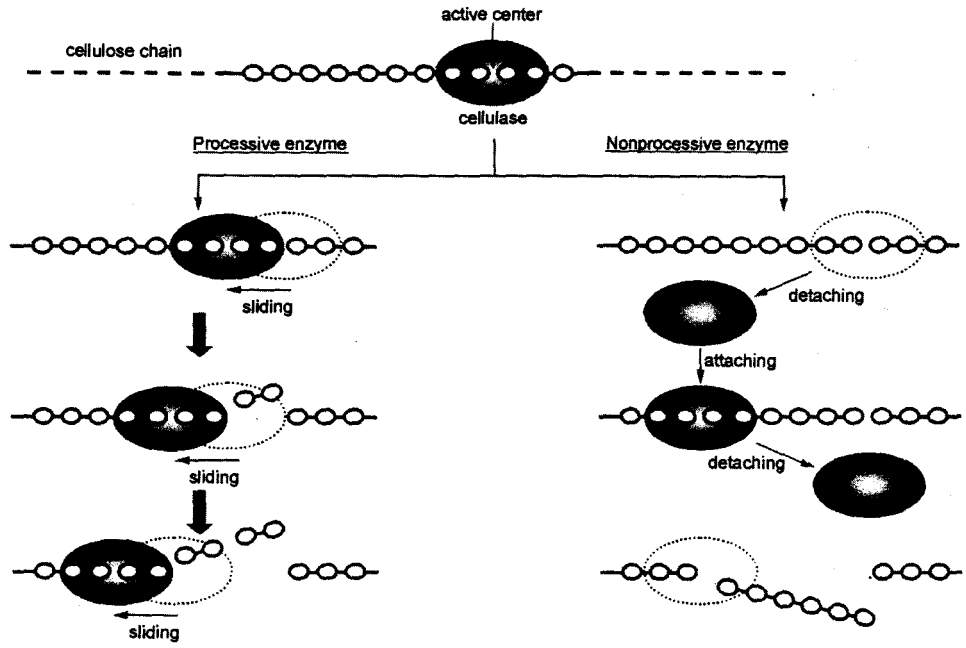

Figure 23 Classification of cellulase into processive and nonprocessive types.

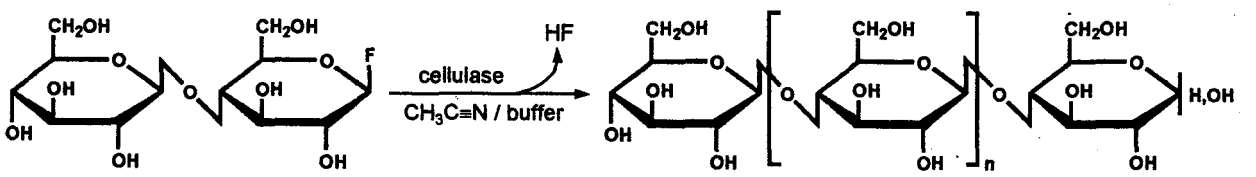

Figure 24 Enzymatic synthesis of cellulose from β-cellobiosyl fluoride in acetonitrile/aqueous buffer mixture.

acids having aromatic rings such as tyrosin or triptophan, and these aromatic rings of the cellulose-binding domains attach to hydrophobic plains of cellulose chains through van der Waals force. The active center of the core domains of cellulase can then attack the cellulose chain. The subsites of the core domains can give some mechanical stress to the cellulose chain, and one of glucose residues of the cellulose chain compulsorily have the unstable boat form. Thus, remarkable reduction of activation energy to hydrolyze cellulose can be achieved [120].

Various types of cellulase have been reported so far, and they have been, for a long time, classified into two types–exo- and endocellulases–depending on whether or not the cellulase can recognize the reducing ends of cellulose chains. Cellobiohydrolase (CBH) and endoglucanase (EG) are then further categorized into two types. However, recent studies revealed that there are no exo-type cellulases, and that all cellulases are included in the endo-type. On the other hand, the following classification are now well accepted: the processive and nonprocessive cellulases on the basis of hydrolysis patterns of cellulose chains (Fig. 23) [121].

C. Thermal Degradation

When cellulose is analyzed by thermogravimetry under nitrogen atmosphere, thermal decomposition starts at 200–270°C, depending on the punty of cellulose samples. The temperature of ignition in the air is in the range of 390–420°C, and the maximum flame temperature reaches 800°C or more. When cellulose is heated at temperatures exceeding 100°C under reduced pressure, levoglucosan (Fig. 22) is obtained in the maximum yield of 70%. When thermal carbonization is applied to cellulosic materials under inactive gas atmosphere, the yields of carbon are lower than the theoretical value (44%) because a part of cellulose is converted to levoglucosan. Yields of carbon can be increased by adding hydrochloric acid, which enhances dewatering rather than the formation of levoglucosan

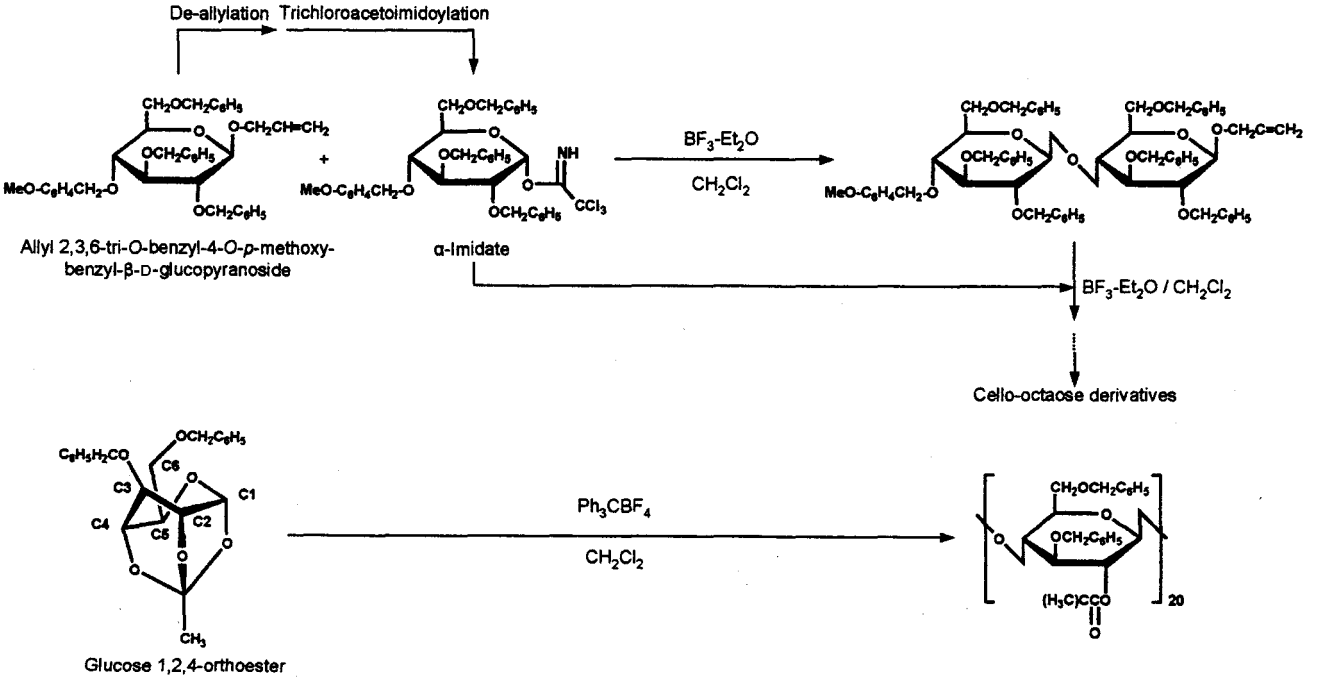

Figure 25 Chemical syntheses of cellulose.

[122]. When cellulose microcrystals, which are obtained from crystalline native celluloses by acid hydrolysis, are carbonized under suitable conditions, carbon nano-lods are obtained [123].

Microwave treatment is one of the heating methods used, in which more homogeneous heating can be achieved, compared with the thermal conduction-type heating. Saccharification of lignocellulosics has been studied from this aspect, and the maximum yield of glucose was reported to be 81% based on theoretical value [124]. Two of the thermal treatments, explosion and laser irradiation treatments, were employed to obtain glucose and levoglucosan. Supercritical water treatment is also one of the heating methods in the presence of acid. Dissociation of water can increase under supercritical conditions, and thus water behaves like an acid catalyst to cellulose. Noncatalytic hydrolysis of cellulose can, therefore, be achieved by supercritical water treatments. The maximum yield of glucose was reported to be in the range of 32–48% [125].

VI. CHEMICAL AND ENZYMATIC SYNTHESES OFCELLULOSE

Although cellulose is one of the naturally occurring polysaccharides, artificial synthesis of cellulose from monomers or dimers has been of scientific interest for a long time. Syntheses of cellulose have recently been succeeded by the following two different principles.

Cellulase hydrolyzes the β-l,4-glucoside bonds of cellulose, and this enzymatic hydrolysis is essentially reversible. Kobayashi et al. [126] successfully carried out cellulose synthesis by using the reversible reaction of cellulase, where a particular substrate, β-cellobiosyl fluoride, was used in an aqueous buffer containing acetonitrile (Fig. 24). The origin and purity of cellulase and combination of the solvent systems influenced the yields of synthesized cellulose and its crystal structure. Cellulase from *Trichoderima viride* gave the highest yield, ca. 54%, of water-insoluble, low-molecular weight cellulose (DP 22), whereas β-glucosidase yielded no cellulose. Generally, the enzymatically synthesized cellulose has the crystal structure of cellulose II, which is the same as that of regenerated or mercerized cellulose. On the other hand, cellulose bearing the crystal structure of cellulose I, which is the same as that of native cellulose, was synthesized in vitro by using a highly purified cellulase component [127].

Cellulose oligomers and low-DP cellulose have been prepared by the following three routes and the successive elimination of the protecting groups at hydroxyl groups: (1) linear synthetic reaction using the imidate method from allyl 2,3,6-tri-*O*-benzyl-4-*O*-p-rnethoxybenzyl-β-D-glucopyranoside, (2) confluent-type reaction between cellotetraose and cellooctaose derivatives using the imidate method, and (3) cationic ring-opening polymerization of glucose 1,2,4-orthoester (Fig. 25). These studies revealed the roles of specific protecting groups at particular hydroxyl positions of the starting materials in regioselective reactions and conformational restrictions for polymerization of carbohydrate monomers [128].

REFERENCES

1. Atalla, R.H. In *Comprehensive Natural Products Chemistry, Carbohydrates*; Pinto, B.M., Ed.; Elsevier: London, 1999; Vol. 3, 529–598.
2. Gardner, K.H.; Blackwell, J. Biopolymers 1974, *13*, 1975.
3. Hebert, J.J.; Muller, L.L. J. Appl. Polym. Sci. 1974, *18*, 3373.
4. Meyer, K.H.; Misch, L. Helv. Chim. Acta 1937, *20*, 232.
5. Hermans, P.H. *Physics and Chemistry of Cellulose Fibers*; Elsevier: New York, 1949.
6. French, A. In *The Structures of Celluloses*, ACS symposium Series 340; Atalla, R.H., Ed.; American Chemical Society: Washington, DC, 1987; 15 pp.
7. Pauling, L. *The Nature of the Chemical Bond*, 3rd Ed.; Cornell University Press: Ithaca, NY, 1960; 65 pp.
8. Woodward, L.A. *Introduction to the Theory of Molecular Vibrations and Vibrational Spectroscopy*; Oxford University Press: Oxford, 1972; 344 pp.
9. Atalla, R.H. Appl. Polym. Symp. 1976, *28*, 659.
10. Pitzner, L.J. *The Vibrational Spectra of the 1,5-anhydropentitols, Doctoral dissertation*; The Institute of Paper Chemistry: Appleton, WI, 1973.
11. Pitzner, L.J.; Atalla, R.H. Spectrochim. Acta 1975, *31A*, 911.
12. Watson, G.M. *The Vibrational Spectra of the Pentitols and Erythritol, Doctoral Dissertation*; The Institute of Paper Chemistry: Appleton, WI, 1974.
13. Edwards, S.L. *The Vibrational Spectra of the Pentose Sugars, Doctoral Dissertation*; The Institute of Paper Chemistry: Appleton, WI, 1976.
14. Williams, R.M. *The Vibrational Spectra of the Inositols, Doctoral Dissertation*; The Institute of Paper Chemistry: Appleton, WI, 1977.
15. Williams, R.M.; Atalla, R.H. J. Phys. Chem. 1984, *88*, 508.
16. Wells, H.A. *The Vibrational Spectra of Glucose, Galactose and Mannose, Doctoral Dissertation*; The Institute of Paper chemistry: Appleton, WI, 1977.
17. Wells, H.A.; Atalla, R.H. J. Mol. Struct. 1990, *224*, 385.
18. Carlson, K.P. *The Vibrational Spectra of the Cellodextrins, Doctoral Dissertation*; The Institute of Paper Chemistry: Appleton, WI, 1978.
19. Wiley, J.H.; Atalla, R.H. Carbohydr. Res. 1987, *160*, 113.
20. Rees, D.A.; Skerret, R.J. Carbohydr. Res. 1968, *7*, 334.
21. Petipas, T.; Oberlin, M.; Mering, J. J. Polym. Sci. C 1963, *2*, 423.
22. Norman, M. Text. Res. J. 1963, *33*, 711.
23. Sarko, A.; Muggli, R. Macromoles 1974, *7*, 486.
24. Chu, S.S.C.; Jeffrey, G.A. Acta. Crystallogr. 1968, *B24*, 830.
25. Ham, J.T.; Williams, D.G. Acta. Crystallogr. 1970, *B29*, 1373.
26. Wilson, E.B., Jr.; Decius, J.C.; Cross, P.c. *Molecular Vibrations*; McGraw-Hill: New York, 1955; 188 pp.
27. Nelson, M.L.; O'Connor, R.T. J. Appl. Polym. Sci. 1964, *8*, 1311.
28. Melberg, S.; Rasmussen, K. Carbohydr. Res. 1979, *71*, 25.
29. Henrissat, B.; Perez, S.; Tvaroska, I.; Winters, w.T. In *The Structures of Celluloses*, ACS symposium Series 340; Atalla, R.H., Ed.; American Chemical Society: Washington, DC, 1987; 38 pp.
30. Atalla, R.H. Adv. Chem. Ser. 1979, *181*, 55.
31. Atalla, R.H.; Gast, J.C.; Sindorf, D.W.; Bartuska, V.J.; Maciel, G.E. J. Am. Chem. Soc. 1980, *102*, 3249.

32. Atalla, R.H. Proceedings of the International Symposium on Wood and Pulping Chemistry, SPCI Rept. No 38, Stockholm 1981, *1*, 57.
33. Atalla, R.H. In *Structure, Function and Biosynthesis of Plant Cell Walls*; Dugger, W.M., Bartinicki-Garcia, S., Eds.; American Society of Plant Physiologists: Rockville, MD, 1984. 381 pp.
34. Atalla, R.H. J. Appl. Pol. Sci., Appl. Pol. Symp. 1983, *37*, 295.
35. Earl, W.L.; VanderHart, D.L. J. Am. Chem. Soc. 1980, *102*, 3251.
36. Earl, W.L.; VanderHart, D.L. Macromoles 1981, *14*, 570.
37. D.L. VanderHart, Deductions about the morphology of wet and wet beaten cellulose from solid state ^{13}C NMR, NBSIR 82-2534.
38. Fyfe, C.A.; Dudley, R.L.; Stephenson, P.J.; Deslandes, Y.; Hamer, G.K.; Marchessault, R.H. J. Am. Chem. Soc. 1983, *105*, 2469.
39. Horii, F.; Hirai, A.; Kitamaru, R. Polym. Bull. 1982, *8*, 163.
40. Maciel, G.E.; Kolodziejski, W.L.; Bertran, M.S.; Dale, B.R. Macromoles 1982, *15*, 686.
41. Gast, J.C.; Atalla, R.H.; McKelvey, R.D. Carbohydr. Res. 1980, *84*, 137.
42. VanderHart, D.L.; Atalla, R.H. Macromoles 1984, *17*, 1465.
43. Atalla, R.H.; VanderHart, D.L. Science 1984, *223*, 283.
44. Howsmon, J.A.; Sisson, W.A. In *Cellulose and Cellulose Derivatives*, Pt. I; Ott, E., Spurlin, H.M., Graffline, M.W., Eds.; Interscience: New York, 1954; 237 pp.
45. Blackwell, J.; Marchessault, H. In *Cellulose and Cellulose Derivatives*, Pt. IV; Bikales, N.M., Segal, L., Eds.; Wiley-Interscience: New York, 1971; 1 pp.
46. VanderHart, D.L.; Atalla, R.H. In *The Structures of Celluloses*, ACS Symposium Series 340; Atalla, R.H., Ed.; American Chemical Society: Washington, DC, 1987; 88 pp.
47. Atalla, R.H.; Whtimore, R.E.; VanderHart, D.L. Biopolymers 1985, *24*, 421.
48. Horii, F.; Yamamoto, H.; Kitamaru, R.; Tanahashi, M.; Higuchi, T. Macromoles 1987, *20*, 2946.
49. Wiley, J.H.; Atalla, R.H. In *The Structures of Celluloses*, ACS Symposium Series 340; Atalla, R.H., Ed.; American Chemical Society: Washington, DC, 1987; 151 pp.
50. Sugiyama, J.; Presson, J.; Chanzy, H. Macromoles 1990, *24*, 4168.
51. Yamamoto, H.; Horii, F.; Odani, H. Macromolecules 1989, *22*, 4130.
52. Sugiyama, J.; Okano, T.; Yamamoto, H.; Horii, F. Macromoles 1990, *23*, 3196.
53. Atalla, R.H.; Hackney, J.; Agarwal, U.P.; Isogai, A. Int. J. Biol. Macromol. *in press*.
54. Bower, D.I.; Maddams, W.F. *The Vibrational Spectroscopy of Polymers*; Cambridge University Press: Cambridge, UK, 1989.
55. Horri, F.; Hirai, A.; Kitamaru, R. *The Structures of Celluloses*, ACS Symposium Series 340; Atalla, R.H., Ed.; American Chemical Society: Washington, DC, 1987; 119 pp.
56. VanderHart, D.L.; Campbell, G.C. J. Magn. Reson. *in press*.
57. Yamamoto, H.; Horii, F. Macromoles 1993, *26*, 1313.
58. Yamamoto, H.; Horii, F.; Odani, H. Macromoles 1989, *22*, 4130.
59. Yamamoto, H.; Horii, F. Macromoles 1993, *26*, 1313.
60. Belton, P.S.; Tanner, S.F.; Cartier, N.; Chanzy, H. Macromoles 1989, *22*, 1615.
61. Yamamoto, H.; Horii, F. Cellulose 1994, *1*, 57.
62. Newman, R.H.; Hemmingson, J.A. Holzforschung 1990, *44*, 351.
63. Newman, R.H.; Hemmingson, J.A. Cellulose 1995, *2*, 95.
64. Newman, R.H. J. Wood Chem. Technol. 1994, *14*, 451.
65. Newman, R.H.; Ha, M.A.; Melton, L.D. J. Agric. Food Chem. 1994, *42*, 1402.
66. Newman, R.H.; Davies, L.M.; Harris, P.J. Plant Physiol. 1996, *111*, 474.
67. Newman, R.H. Cellulose 1997, *4*, 269.
68. Lenholm, H.; Larsson, T.; Iversen, T. Carbohydr. Res. 1994, *261*, 119.
69. Lennholm, H.; Larsson, T.; Iversen, T. Carbohydr. Res. 1994, *261*, 119.
70. Larsson, T.; Westermark, U.; Iversen, T. Carbohydr. Res. 1995, *278*, 339.
71. Larsson, T.; Wickholm, K.; Iversen, T. Carbohydr. Res. 1997, *302*, 19.
72. Hock, C.W. In *Cellulose and Cellulose Derivatives*, Pt. I; Ott, E., Spurlin, H.M., Grafflin, M.W., Eds.; Interscience: New York, 1954; 347 pp.
73. Morehead, F.F. In *Cellulose and Cellulose Derivatives*, Pt. IV; Bikales, N.M., Segal, L., Eds.; Wiley-Interscience: New York, 1971; 213 pp.
74. Preston, R.D. *The Physical Biology of Plant Cell Walls*; Chapman & Hall: London, 1974.
75. Hieta, K.; Kuga, S.; Usuda, M. Biopolymers 1984, *23*, 1807.
76. Chanzy, H.; Henrissat, B. FEBS Lett. 1985, *184*, 285.
77. Maurer, A.; Fengel, D. Holz als Roh- und Werkstoff 1992, *50*, 493.
78. Sugiyama, J.; Harada, H.; Fujiyoshi, Y.; Uyeda, N. Mokuzai Gakkaishi 1984, *30*, 98.
79. Sugiyama, J.; Harada, H.; Fujiyoshi, Y.; Uyeda, N. Mokuzai Gakkaishi 1985, *31*, 61.
80. Sugiyama, J.; Harada, H.; Fujiyoshi, Y.; Uyeda, N. Planta 1985, *166*, 161.
81. Frey-Wyssling, A. *The Plant Cell Wall*; Gebruder Borntrager: Berlin, 1976.
82. Sugiyama, J.; Okano, T.; Yamamoto, H.; Horii, F. Macromoles 1990, *23*, 3196.
83. Honjo, G.; Watanabe, M. Nature 1958, *181*, 326.
84. Sugiyama, J.; Vuong, R.; Chanzy, H. Macromoles 1991, *24*, 4168.
85. Roche, E.; Chanzy, H. J. Biol. Macromol. 1981, *3*, 201.
86. Ellefsen, 0.; Tonessen, B.A. In *Cellulose and Cellulose Derivatives*, Pt. IV; Bikales, N.M., Segal, L., Eds.; Wiley-Interscience: New York, 1971; 151 pp.
87. Chanzy, H.; Henrissat, B.; Vincendon, M.; Tanner, S.; Belton, P.S. Carbohydr. Res. 1987, *160*, 1.
88. Atalla, R.H.; Dimick, B.E.; Nagel, S.C. In *Cellulose Chemistry and Technology*; Arthur, J.C. Jr., Ed.; ACS Symp. Series No. 40, American Chemical Society: Washington, DC, 1977; 30 pp.
89. Atalla, R.H.; Ellis, J.D.; Schroeder, L.R. J. Wood Chem. Technol. 1984, *4*, 465.
90. Chanzy, H.; Imada, K.; Mollard, A.; Vuong, R.; Barnoud, F. Protoplazma 1979, *100*, 303.
91. Bertoniere, N.R.; Zeronian, S.H. In *The Structures of Celluloses*, ACS Symposium Series 340; Atalla, R.H., Ed.; American Chemical Society: Washington, DC, 1987; 255 pp.
92. Rowland, S.P.; Roberts, E.J. J. Pol. Sci. A-1 1972, *10*, 2447.
93. Nickerson, R.F. Text. Res. J. 1951, *21*, 195.
94. Rowland, S.P.; Roberts, E.J.; Wade, C.P. Text. Res. J. 1969, *39*, 530.
95. Rowland, S.P. In *Modified Cellulosics*; Rowell, R.M., Young, R.A., Eds.; Academic Press: New York, 1978; 147 pp.
96. Rowland, S.P.; Roberts, E.J.; Bose, J.L. J. Pol. Sci. A-1 1971, *9*, 1431.
97. Rowland, S.P.; Roberts, E.J.; Bose, J.L.; Wade, C.P. J. Pol. Sci. A-1 1971, *9*, 1623.

98. Mann, J.; Marinan, H.J. J. Polym. Sci. 1958, *32*, 357.
99. Zeronian, S.H.; Coole, M.L.; Alger, K.W.; Chandler, J.M. J. Appl. Pol. Sci., Appl. Pol. Symp. 1983, *37*, 1053.
100. Stone, J.E.; Scallan, A.M. Pulp Pap. Mag. Can. 1968, *69*, 69.
101. Stone, J.E.; Treiber, E.; Abrahamson, E. TAPPI 1969, *28*, 139.
102. Bell, R.P. *The Proton in Chemistry*; Cornell University Press: Ithaca, NY, 1973.
103. Johnson, D.C.; Nicholson, M.D.; Haigh, F.C. Appl. Polym. Symp. 1976, *28*, 931.
104. Johnson, D.C.; Nicholoson, M.D. Cellul. Chem. Technol. 1977, *11*, 349.
105. Isogai, A. Chemical modification of cellulose. In *Wood and Cellulosic Chemistry*; Hon, D.N.-S., Shiraishi, N., Eds.; Mercer Dekker: New York, 2000, 599–625.
106. Isogai, A.; Atalla, R.H. Dissolution of cellulose in aqueous NaOH solutions. Cellulose 1998, *5*, 309–319.
107. Kamide, K.; Okajima, K.; Kowsaka, K. Dissolution of natural cellulose into aqueous alkali solutions: Role of supermolecular structure of cellulose. Polym. J. 1992, *24*, 71–86.
108. Isogai, A.; Atalla, R.H. Preparation of cellulose–chitosan polymer blends. Carbohydr. Polym. 1992, *19*, 25–28.
109. Turbak, A.F., El-Kafrawy, A., Snyder, F.W., Jr., Auerbach, A.B., Solvent system for cellulose, U.S. Pat., 4302252 (1981).
110. Schult, T.; Hjerde, T.; Optun, O.I.; Kleppe, P.J.; Moe, S. Characterization of cellulose by SEC-MALLS. Cellulose 2002, *9*, 149–158.
111. Okajima, K.; Yamane, C. Cellul. Commun. 1997, *4*, 7–12.
112. Saka, S.; Takahashi, K.; Matsumura, H. Effects of solvent addition to acetylation medium on cellulose triacetate prepared from low-grade hardwood dissolving pulp. J. Appl. Polym. Sci. 1998, *69*, 1445–1449.
113. Jumel, K.; Harding, S.E.; Mitchell, J.R.; To, K.-M.; Hayter, I.; O'Mullane, J.E.; Ward-Smith, S. Carbohydr. Polym. 1996, *29*, 105–109.
114. Tanaka, R.; Meadows, J.; Phillips, G.O.; Williams, P.A. Viscometric and spectroscopic studies on the solution behavior of hydrophobically modified cellulosic polymers. Carbohydr. Polym. 1990, *12*, 443–459.
115. Isogai, A.; Ishizu, A.; Nakano, J. Preparation of tri-*O*-alkylcelluloses by the use of a non-aqueous cellulose solvent and their physical characteristics. J. Appl. Polym. Sci. 1986, *31*, 341–352.
116. Kondo, T.; Gray, D.G. The preparation of *O*-methylcellulosese and *O*-ethylcelluloses having controlled distribution of substituents. Carbohydr. Res. 1991, *220*, 173–183.
117. de Nooy, A.E.J.; Besemer, A.C.; Bekkum, H. Highly selective nitroxyl radical-mediated oxidation of primary alcohol groups in water-soluble glucans. Carbohydr. Res. 1995, *269*, 89–98.
118. Isogai, A.; Kato, Y. Preparation of polyuronic acid from cellulose by TEMPO-mediated oxidation. Cellulose 1998, *5*, 153–164.
119. Kato, Y.; Habu, N.; Yamaguchi, J.; Kobayashi, Y.N.; Shibata, I.; Isogai, A.; Samejima, M. Biodegradation of β-1,4-linked polyglucuronic acid (cellouronic acid). Cellulose 2002, *9*, 75–81.
120. Henrissat, B. Cellulases and their interaction with cellulose. Cellulose 1994, *1*, 169–196.
121. Davies, G.; Henrissat, B. Structures and mechanisms of glycosyl hydrolases. Structure 1995, *3*, 853–859.
122. Kim, D.Y.; Nishiyama, Y.; Wada, M.; Kuga, S. High-yield carbonization of cellulose by sulfuric acid impregnation. Cellulose 2001, *8*, 29–33.
123. Kuga, S.; Kim, D.Y.; Nishiyama, Y.; Brown, R.M. Nanofibrillar carbon from native cellulose. Mol. Cryst. Liq. Cryst. 2002, *387*, 237–243.
124. Azuma, J.; Asai, T.; Isaka, M.; Koshijima, T. Microwave irradiation of lingocellulosic materials. 5. Effects of microwave irradiation on enzymatic susceptibility of crystalline cellulose. J. Ferment. Technol. 1985, *63*, 529–536.
125. Saka, S.; Ueno, T. Chemical conversion of various celluloses to glucose and its derivatives in supercritical water. Cellulose 1999, *6*, 177–191.
126. Kobayashi, S.; Kashiwa, K.; Kawasaki, T.; Shoda, S. Novel method for polysaccharide synthesis using an enzyme—The first in vitro synthesis of cellulose via a non-biosynthetic path utilizing cellulase as catalyst. J. Am. Chem. Soc. 1991, *113*, 3079–3084.
127. Lee, J.H.; Brown, R.M.; Kuga, S.; Shoda, S.; Kobayashi, S. Assembly of synthetic cellulose I. Proc. Natl. Acad. Sci. U. S. A. 1994, *91*, 9195.
128. Nakatsubo, F.; Kamitakahara, H.; Hori, M. Cationic ring-opening polymerization of 3,6-di-*O*-benzyl-alpha-D-glucose 1,2,4-orthopivalate and the first chemical synthesis of cellulose. J. Am. Chem. Soc. 1996, *118*, 1677–1681.

POLYSACCHARIDES

STRUCTURAL DIVERSITY AND FUNCTIONAL VERSATILITY

SECOND EDITION

SEVERIAN DUMITRIU
University of Sherbrooke
Quebec, Canada

MARCEL DEKKER NEW YORK

The first edition was published as ***Polysaccharides; Structural Diversity and Functional Versatility,*** edited by Severian Dumitriu (Marcel Dekker. Inc., 1998).

Library of Congress Cataloging-in-Publication Data
A catalog record for this book is available from the Library of Congress

ISBN: 0-8247-5480-8

This book is printed on acid-free paper.

Headquarters
Marcel Dekker
270 Madison Avenue, New York, NY 10016, U.S.A.
tel: 212-696-9000; fax: 212-685-4540

Distribution and Customer Service
Marcel Dekker
Cimarron Road, Monticello, New York 12701, U.S.A.
tel: 800-228-1160; fax: 845-796-1772

World Wide Web
http://www.dekker.com

The publisher offers discounts on this book when ordered in bulk quantities. For more information, write to Special Sales/Professional Marketing at the headquarters address above.

Current printing (last digit):

10 9 8 7 6 5 4 3 2 1

PRINTED IN THE UNITED STATES OF AMERICA